

CHARACTERIZATION OF UVB INDUCIBLE GENE EXPRESSION IN
XIPHOPHORUS SKIN

THESIS

Presented to the Graduate Council of
Texas State University–San Marcos
in Partial Fulfillment
of the Requirements

for the Degree

Master of SCIENCE

by

Kevin P. Downs, B.S.

San Marcos, Texas
May 2013

CHARACTERIZATION OF UVB INDUCIBLE GENE EXPRESSION IN
XIPHOPHORUS SKIN

Committee Members Approved:

Ronald B. Walter, Chair

Rachell E. Booth

Corina Maeder

Approved:

J. Michael Willoughby
Dean of the Graduate College

COPYRIGHT

by

Kevin P. Downs

2013

FAIR USE AND AUTHOR'S PERMISSION STATEMENT

Fair Use

This work is protected by the Copyright Laws of the United States (Public Law 94-553, section 107). Consistent with fair use as defined in the Copyright Laws, brief quotations from this material are allowed with proper acknowledgment. Use of this material for financial gain without the author's express written permission is not allowed.

Duplication Permission

As the copyright holder of this work I, Kevin P. Downs, authorize duplication of this work, in whole or in part, for educational or scholarly purposes only.

ACKNOWLEDGEMENTS

I would like to acknowledge research lab members at Texas State University-San Marcos, particularly Dr. Tzintzuni Garcia, Dr. Yingjia Shen, and Dr. Vagmita Pabuwal for their assistance with the bioinformatics portion of this project and Amanda Pasquali and Mikki Boswell for their help in the laboratory. I also want to thank members of the *Xiphophorus* genetic stock center, particularly Markita Savage, for additional laboratory assistance. I would like to acknowledge Dr. David Mitchell from MD Anderson at Science Park for providing me with the research animals used in this project and laboratory training in addition to sharing his knowledge on the subject of photobiology and photochemistry with me. I must also thank my two thesis committee members, Dr. Rachell Booth and Dr. Corina Maeder for their constructive feedback during the writing process. Most of all I would like to acknowledge my research advisor Dr. Ronald Walter for allowing me to be a part of his research group since 2009 and providing me with guidance not only in the laboratory but also in life.

This manuscript was submitted on April 3, 2013.

TABLE OF CONTENTS

	Page
ACKNOWLEDGEMENTS	v
LIST OF TABLES	vii
LIST OF FIGURES.....	ix
ABSTRACT	xi
CHAPTER	
1. INTRODUCTION.....	1
2. MATERIALS AND METHODS	18
3. DETERMINATION OF UVB-INDUCED DNA PHOTOPRODUCT FORMATION AND LIGHT INDUCED MODULATION OF GENE EXPRESSION IN <i>XIPHOPHORUS SKIN</i>	31
4. IDENTIFICATION OF BIOLOGICAL PATHWAYS MODULATED BY UVB AND/OR PRL EXPOSURE IN <i>X. MACULATUS</i> JP 163 B SKIN	52
LITERATURE CITED	91

LIST OF TABLES

Table	Page
1-1: Photolyase sequences that have been identified in multiple organisms by genomic resources	11
2-1: Primers used for gene expression analysis by quantitative real-time PCR.....	30
3-1: Radioimmunoassay detection of CPDs in <i>Xiphophorus</i> skin	34
3-2: Radioimmunoassay detection of (6-4)PDs in <i>Xiphophorus</i> skin.....	36
3-3: Separation of significant up-regulated transcripts by fold change values	43
3-4: Separation of significant down-regulated transcripts by fold change values	44
4-1: DAVID functional analysis clustering of up-regulated genes in UVB exposed skin of <i>X. maculatus</i> Jp 163 B	55
4-2: List of genes placed within multiple biological categories after DAVID functional analysis clustering of up-regulated genes in UVB exposed skin of <i>X. maculatus</i> Jp 163 B.....	56
4-3: DAVID functional analysis clustering of down-regulated genes in UVB exposed skin of <i>X. maculatus</i> Jp 163 B	58
4-4: List of genes placed within multiple biological categories after DAVID functional analysis clustering of down-regulated in UVB exposed skin of <i>X. maculatus</i> Jp 163 B.....	59
4-5: DAVID functional analysis clustering of up-regulated genes in PRL exposed skin of <i>X. maculatus</i> Jp 163 B	62
4-6: List of genes placed within multiple biological categories after DAVID functional analysis clustering of up-regulated genes in PRL exposed skin of <i>X. maculatus</i> Jp 163 B.....	63

4-7: DAVID functional analysis clustering of down-regulated genes in PRL exposed skin of <i>X. maculatus</i> Jp 163 B	65
4-8: List of genes placed within multiple biological categories after DAVID functional analysis clustering of down-regulated genes in PRL exposed skin of <i>X. maculatus</i> Jp 163 B	66
4-9: DAVID functional analysis clustering up-regulated genes in UVB + PRL exposed of <i>X. maculatus</i> Jp 163 B	69
4-10: List of genes placed within multiple biological categories after DAVID functional analysis clustering of up-regulated genes in UVB + PRL exposed skin of <i>X. maculatus</i> Jp 163 B.....	70
4-11: DAVID functional analysis clustering of down-regulated genes in UVB + PRL exposed skin of <i>X. maculatus</i> Jp 163 B.....	72
4-12: List of genes placed within multiple biological categories after DAVID functional analysis clustering of down-regulated genes in UVB + PRL exposed skin of <i>X. maculatus</i> Jp 163 B.....	73

LIST OF FIGURES

Figure	Page
1-1: Penetrance of UVC, UVB, and UVA through the atmosphere and skin.....	3
1-2: Chemical structures of the cyclobutane pyrimidine dimer (CPD) and pyrimidine (6-4) pyrimidinone photoproduct [(6-4)PD].....	5
1-3: Outline of Eukaryotic Nucleotide excision repair (NER).....	7
1-4: Proposed mechanisms for CPD and (6-4)PD photolyases.....	10
1-5: A <i>Xiphophorus</i> melanoma model hybridization scheme.....	15
2-1: Images of <i>Xiphophorus</i> fish used within this study.....	19
2-2: Experimental light exposure set-up.....	22
2-3: Diagram of radioimmunoassay protocol for the quantification of CPDs and (6-4)PDs in DNA extracted from mammalian cells and tissues.....	24
2-4: Overview of Illumina RNA sequencing.....	26
3-1: Radioimmunoassay detection of CPDs in <i>Xiphophorus</i> skin.....	35
3-2: Radioimmunoassay detection of (6-4)PDs in <i>Xiphophorus</i> skin.....	37
3-3: Transcript expression differences in UVB exposed vs. unexposed skin from <i>X. maculatus</i> Jp 163 B determined by DESeq analysis.....	39
3-4: Transcript expression differences in UVB + PRL exposed vs. unexposed skin from <i>X. maculatus</i> Jp 163 B determined by DESeq analysis.....	40
3-5: Transcript expression differences in PRL exposed vs. unexposed skin from <i>X. maculatus</i> Jp 163 B determined by DESeq analysis.....	41

3-6: Venn diagram comparison of significant up-regulated genes in <i>X. maculatus</i> Jp 163 B skin after UVB exposure, UVB + PRL exposure, or PRL exposure	46
3-7: Venn diagram comparison of significant down-regulated genes in <i>X. maculatus</i> Jp 163 B skin after UVB exposure, UVB + PRL exposure, or PRL exposure	47
4-1: STRING analysis of significant up-regulated genes in UVB exposed skin of <i>X. maculatus</i> Jp 163 B	57
4-2: STRING analysis of significant down-regulated genes in UVB exposed skin of <i>X. maculatus</i> Jp 163 B	60
4-3: STRING analysis of significant up-regulated genes in PRL exposed skin of <i>X. maculatus</i> Jp 163 B	64
4-4: String analysis of significant down-regulated genes in PRL exposed skin of <i>X. maculatus</i> Jp 163 B	67
4-5: STRING analysis of significant up-regulated genes in UVB + PRL exposed skin of <i>X. maculatus</i> Jp 163 B	71
4-6: STRING analysis of significant of down-regulated genes in UVB + PRL exposed skin of <i>X. maculatus</i> Jp 163 B	74
4-7: Quantitative real-time PCR analysis of verification of RNA-Seq data	76

ABSTRACT

CHARACTERIZATION OF UVB INDUCIBLE GENE EXPRESSION IN *XIPHOPHORUS* SKIN

by

Kevin P. Downs, B.S.

Texas State University-San Marcos

May 2013

SUPERVISING PROFESSOR: RONALD B. WALTER

Hybrids between select *Xiphophorus* species have served as experimental models for UVB induced melanomagenesis. Photobiological responses observed in *Xiphophorus* UV inducible melanoma models support a role for DNA damage in carcinogenesis. For example, UVB induced melanomas in *Xiphophorus* backcross hybrids are reduced to near background levels by exposing fish to visible light, presumably to promote photoenzymatic repair (PER) of UV photoproducts. Although this biological endpoint has been well studied, little is known about the initial molecular genetic events of UVB exposure in *Xiphophorus* skin and how this response may be modulated by photoreactivating light (PRL).

Here we report RNAseq results from adult *X. maculatus* exposed to UVB (6.4 kJ) or UVB plus PRL (2 hrs), where total RNA was isolated from skin after 4 hrs in the dark to allow time for gene expression. Concurrent DNA isolation allowed radioimmunoassay to quantify the major UVB photoproducts, cyclobutane pyrimidine dimers (CPDs) and pyrimidine (6-4) pyrimidone photoproducts (6-4PDs).

Skin RNA was sequenced using the Illumina High-Seq platform (100 bp, PE). RNAseq reads were mapped to an *X. maculatus* reference transcriptome using Bowtie and relative gene expression levels compared with DESeq. Blast2GO analysis was used to assign genes functional ontology groups. In *X. maculatus*, genes involved in critical molecular processes such as transcription, DNA repair, and response to cellular stress displayed significantly modulated levels of expression whether PRL was present after UVB exposure or not. These expression patterns, in UVB vs. PRL exposed skin, hallmark wavelength dependent antagonistic regulatory signaling and biochemical pathways.

CHAPTER 1

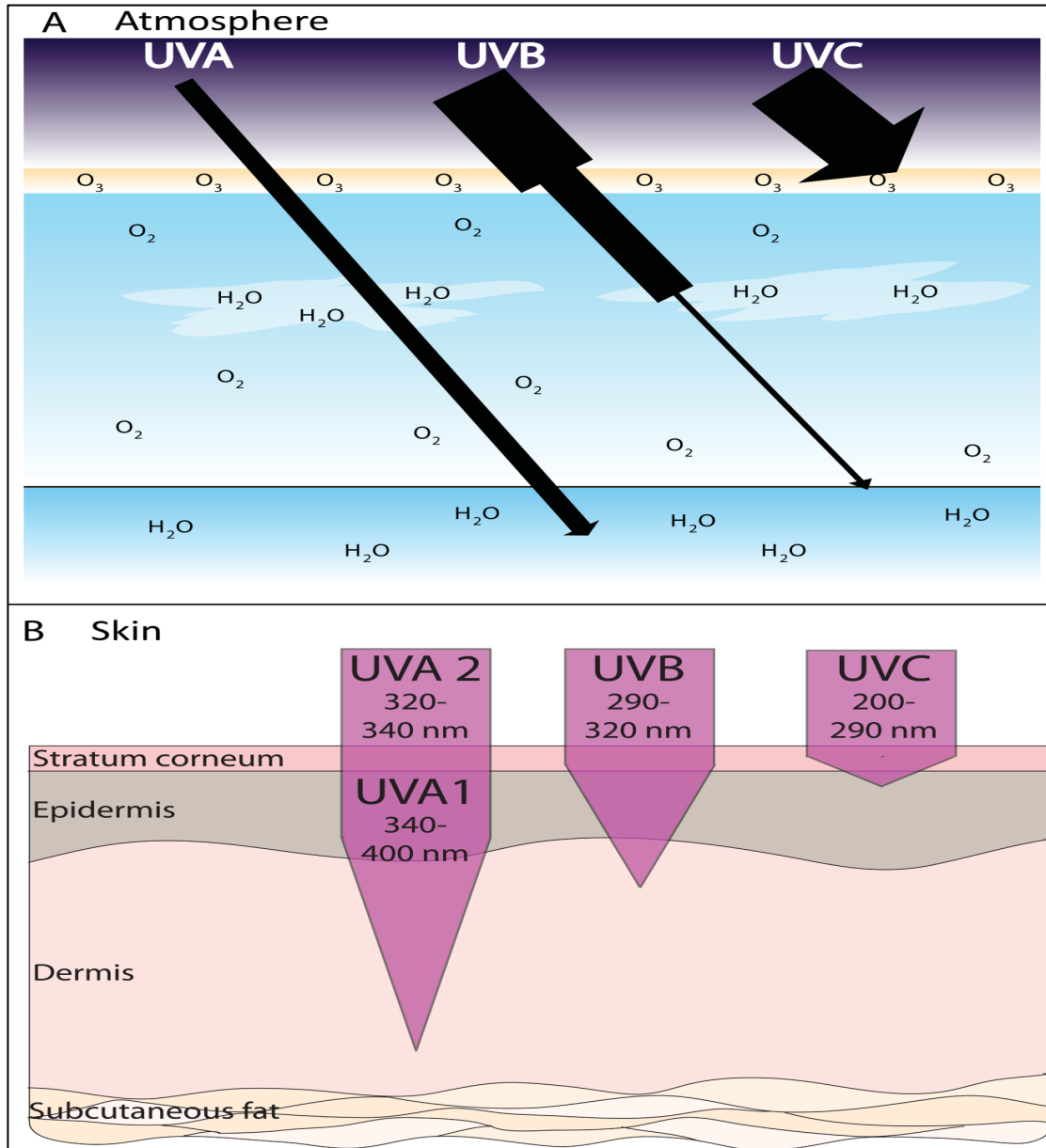
INTRODUCTION

Exploration into the detrimental impact of solar ultraviolet (UV) radiation on all living organisms dates back nearly a century and remains an intensely studied topic of interest to scientists in many fields. UV light can be divided into three major components known as UVC (240-280 nm), UVB (280-320 nm), and UVA (340-400 nm). In considering biological effects it is important to note that wavelength and energy are inversely proportional. Therefore, although UVC spans shorter wavelengths than UVB and UVA, it possesses far greater energy and exhibits less ability to penetrate biological materials (Figure 1-1). Solar UV light that reaches the earth's surface is mostly UVA (90-95%) and UVB (5-10%). All UVC and a small amount of the lower UVB wavelengths are excluded from the earth's surface due to absorption by stratospheric ozone (McKenzie *et al.*, 2003). An important property of UV radiation that separates it from the visible spectrum is that UV light can ionize molecules and thereby induce chemical reactions. This is important when considering cellular components such as DNA that can become damaged after UV exposure of the skin (Friedberg *et al.*, 1995). Increased UV exposure in humans is most notably associated with an increased development of skin cancer. The incidence rate for melanoma, the most deadly form of skin cancer, has continually risen over the years despite the development of sunscreens and public health efforts that promote the avoidance of prolonged sun exposure

(Rigel *et al.*, 1987). Thus, it is likely the etiology of melanoma may minimally involve physical, environmental, behavioral, and genetic components and as a result is a complex disease that remains poorly understood.

Pioneering studies during the first half of the 20th century provided the earliest evidence for the relative effects that exposure to different UV wavelengths may have on organisms. UV light was first investigated for its ability to inhibit the growth of bacteria and inactivate viruses, particularly at the shorter UVC and UVB wavelengths (Hollaender *et al.*, 1935). In 1928 Gates correlated the lethal effects of UV to those wavelengths corresponding to the absorption spectrum of nucleic acids, with a maximum around 260 nm (Gates 1928). Since, purines and pyrimidines were known to be the component of DNA responsible for an absorption maximum at 260 nm, investigations of the effects of UV exposure on DNA quickly followed. Utilizing a simple set-up of a quickly frozen solution of thymine and a germicidal (UVC) low-pressure mercury lamp, Beaukers in 1958 identified the formation of thymine dimers within irradiated samples (Beaukers *et al.*, 1958). Evidence that these UV induced thymine dimers in DNA resulted in biological damage was later provided by Setlow in 1962, marking our earliest understanding on the consequences of UV induced DNA photoproduct formation in cells (Setlow *et al.*, 1962).

DNA photoproducts form due to the direct absorption of UV energy by double bonds present within DNA bases. Wavelengths corresponding to solar UV that are sufficient in forming them fall largely within the UVB spectrum. The two major photoproducts that arise in DNA after UVB exposure are cyclobutane pyrimidine dimers (CPDs) and the pyrimidine (6-4)pyrimidinone dimer [(6-4)PD] between adjacent bases.

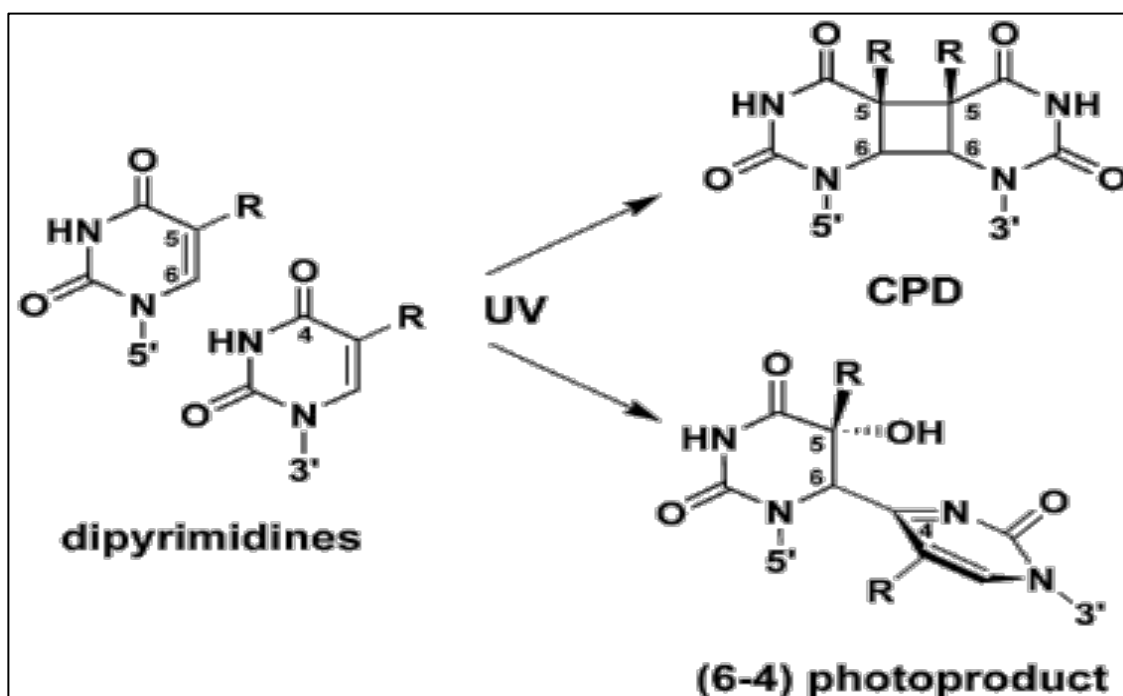


Source: Maverakis *et al.* 2010

Figure 1-1: Penetrance of UVC, UVB, and UVA through the atmosphere and skin. A) Nearly 90% of UVB and all of UVC is absorbed by O₃, O₂, and H₂O in the earth's atmosphere. UVA makes up 95% of the solar UV radiation that reaches the earth surface. B) With its longer wavelengths, UVA is able to penetrate deeper into the skin than UVB, although its lower energy poses less damage to cellular components such as DNA.

CPDs arise due to the formation of a four membered ring structure involving C5 and C6 of adjacent bases, whereas (6-4)PDs are formed through a noncyclic bond formation between C6 (of the 5'-end) and C4 (of the 3'-end) of neighboring bases (Figure 1-2; Wang 1976). The (6-4)PD can undergo further conversion to its Dewar valence isomer form upon exposure to long wavelengths UV (UVA; Lee *et al.*, 2000). Formation of CPDs, relative to (6-4)PDs, in DNA exposed to UVB typically exists at a ratio of about 3:1; however, exceptions exist that are contingent upon DNA sequence and methylation status. Both types of photoproducts affect the spatial structure of DNA and thus contribute to the ability of these DNA lesions to inhibit replication and gene transcription. The bases within the CPD are stacked quasi-parallel to each other and produce a 7° bend in the DNA helix. In contrast, the (6-4)PD produces a 43° bend in the DNA helix with the 3' base lying at 90° relative to the 5' base. The greater distortion imposed on the DNA helix by the (6-4)PD results in it being a very effective block of replication and transcription machinery compared to the CPD (Mitchell *et al.*, 1989).

In order to avoid the consequences of UV photoproduct accumulation within DNA, organisms have evolved DNA repair mechanisms for their removal. Nucleotide excision repair (NER) is central for the repair of DNA photoproducts and is one of the most versatile repair systems in organisms, being highly conserved among prokaryotes and eukaryotes. NER is a repair system that is able to act on an array of DNA lesions that cause bulky adducts or produce major structural changes, such as CPDs and (6-4)PDs, in addition to some forms of oxidative damage and DNA-intrastrand crosslinks. This process was first described in the mid 1960's when Richard Setlow discovered that following exposure to UV light *E. coli* could produce small pieces of DNA, excised



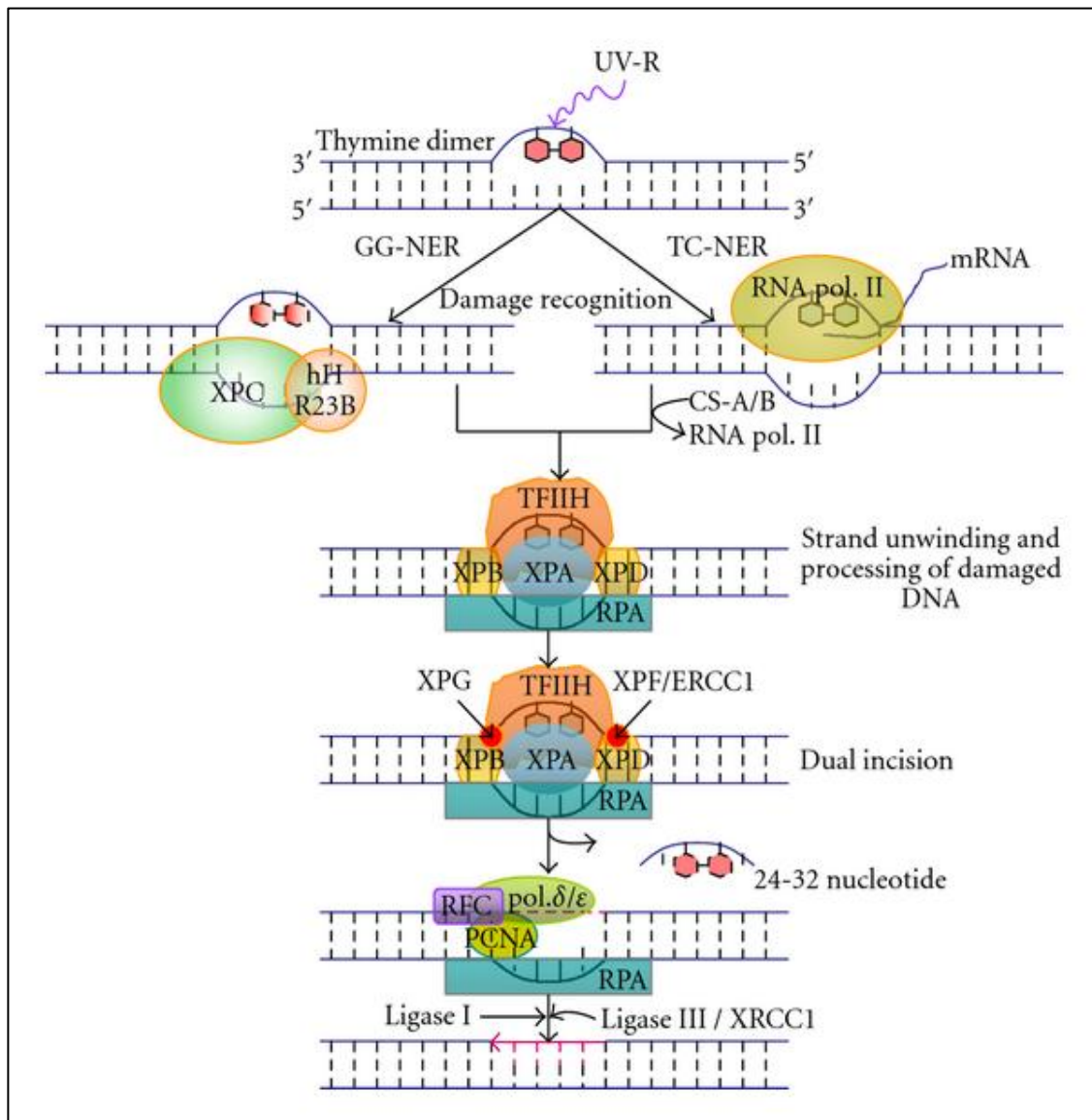
Source: Li *et al.*, 2006

Figure 1-2: Chemical structures of the cyclobutane pyrimidine dimer (CPD) and pyrimidine (6-4) pyrimidinone photoproduct [(6-4)PD]. CPDs form a four membered ring structure involving C5 and C6 of adjacent bases. (6-4)PDs are formed through a noncyclic bond formation between C6 (of the 5'-end) and C4 (of the 3'-end) of neighboring bases.

from their genomes, carrying UV induced lesions such as pyrimidine dimers (Setlow *et al.*, 1964). Isolation of three mutant strains of *E. coli* defective in this process (designated *uvrA*, *uvrB*, and *uvrC*) and mapping the mutant genes to various unique genomic locations provided evidence that multiple gene products were involved in CPD excision (Pettijohn *et al.*, 1964). It is now known that in prokaryotes such as *E. coli*, NER is carried out by about six proteins *UvrA*, *B*, and *C* (ABC-complex, which shows excinuclease activity), *UvrD* (helicase II), DNA polymerase I (pol. I) and DNA ligase (Friedberg *et al.*, 1995).

Eukaryotic NER differs from prokaryotic NER in the numbers of proteins involved and the array of damage recognized, but after damage recognition and repair protein recruitment the damage excision mechanisms are quite similar. In eukaryotes, NER requires 30-40 proteins involved in DNA damage recognition, excision, synthesis, ligation and regulation (Friedberg 2003). NER in eukaryotes can be further subdivided into two differentially regulated subpathways; (1) a pathway responsible for repair of lesions over the entire genome, termed *global genome repair* (GGR), and (2) a separate pathway that repairs lesions present within actively transcribed DNA strands, called *transcription-coupled repair* (TCR).

The core proteins making up NER machinery include XPA and RPA, subunits of the TFIIH general transcription factor (particularly XPB and XPD proteins), the XPC-hHR23B complex (TCR), the XPG nuclease, and the ERCC1-XPF nuclease (Wood 2010; Figure 1-3). In mammalian cells the XPC-hHR23B complex is involved in damage recognition, initiating the NER process in inactive DNA (i.e., GGR). and promoting XPA binding to the damaged site. In actively transcribed DNA (TCR), damage recognition



Source: Rastogi *et al.*, 2010

Figure 1-3: Outline of Eukaryotic Nucleotide excision repair (NER).

NER consists of a linear sequence of reactions that repair UV-induced DNA lesions. Damage recognition for GGR occurs via HR23B/XPC and damage recognition for TCR occurs via RNA pol II arrest and the coupling factors CSA and CSB. XPA interacts with TFIIH, facilitating unwinding by the XPB and XPD members of TFIIH. XPG is then bound through interaction with TFIIH to cleave 3' to the dimer, followed by XPF/ERCC1, which interacts with XPA and cleaves on the 5' side. The cut segment is released and the patch is then resynthesized by polymerase, PCNA and ligase.

occurs via recruitment of the CSA and CSB proteins that form a complex with RNA pol II. After assembly of the other repair proteins, the XPC-hHR23B complex or CSA-CSB complex dissociates, the XPG protein cuts 3' to the lesion and the ERCC1-XPF heterodimer cuts 5' to the lesion. The nuclease complex is released with the 27-30 nucleotide single strand fragment by the action of transcription factor TFIIH after which DNA Pol δ , PCNA, and ligase fills in the remaining gap (Wood 2010).

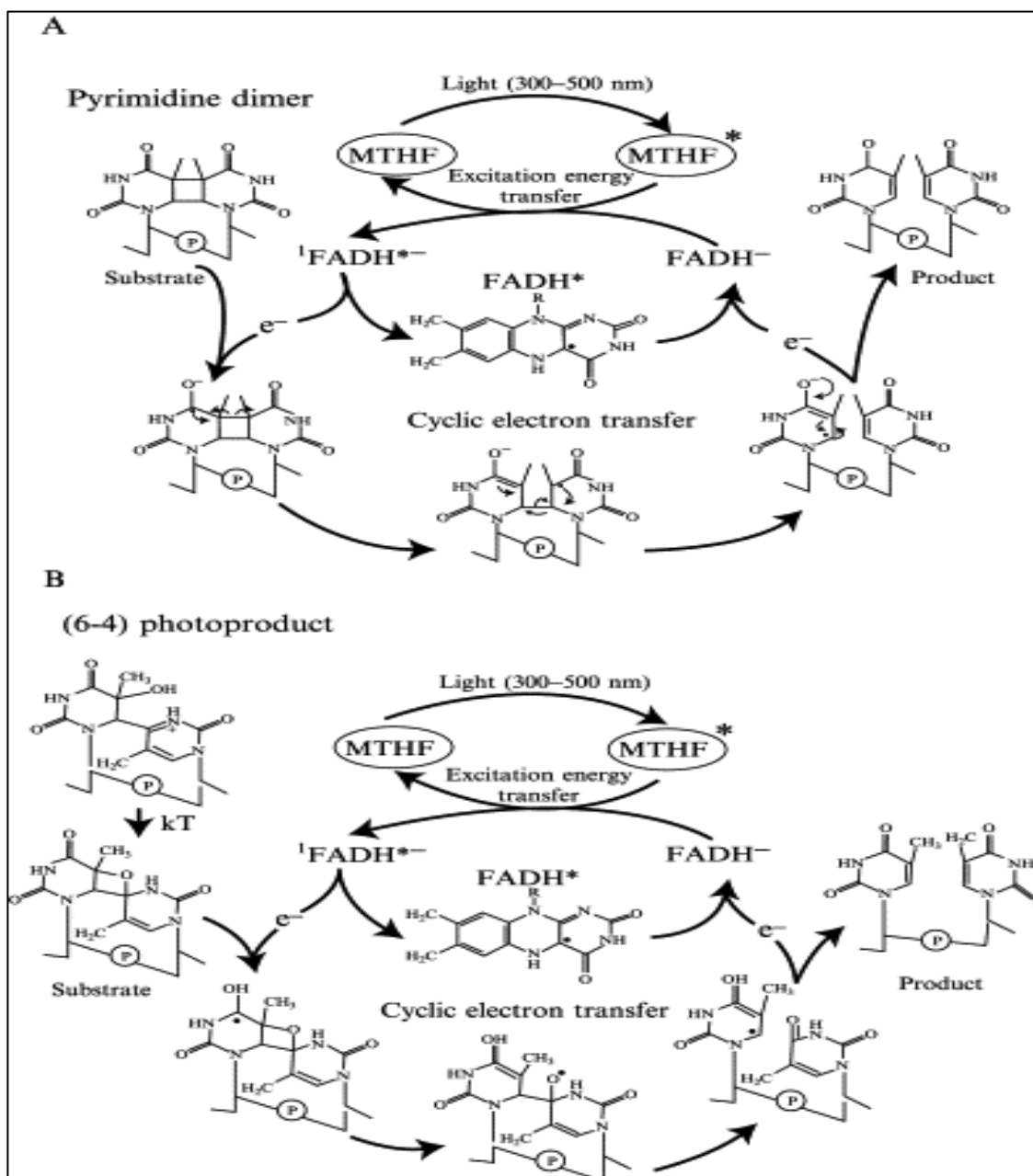
For repair of UV damage, both CPDs and (6-4)PDs are thought to be removed by the same NER proteins, however, the relative repair efficiency of each of these lesions varies considerably in mammalian cells. Previous work in both human and Chinese hamster (CHO) cells has demonstrated that elimination of the (6-4)PDs is at least fivefold faster than removal of CPDs (Mitchell *et al.*, 1989). This is thought to be largely attributed to the greater helical distortion imposed by the (6-4)PD compared to that of the CPD that aids (6-4)CPD detection and excision. However, the CPD photolesion is considered more mutagenic due to its greater repair time and thus an increased probability of misrepair by other systems (i.e., gene conversion) and/or being encountered by replicative machinery prior to removal. Unrepaired CPDs may result in two signature mutations (C > T, CC > TT) that have been identified in the TP53 tumor suppressor gene (p53 protein) and associated with basal cell and squamous cell carcinomas (Ziegler *et al.*, 1993). These UV mutational signatures in critical genes suggest that UV photoproduct may be involved in skin carcinogenesis, however, the precise mechanisms that bring about this association remain controversial.

Photoenzymatic repair (PER) is another mechanism by which certain organisms can directly repair CPDs and (6-4)PDs. PER is an extremely efficient process that results

in direct reversal of DNA photoproducts. PER requires only a single enzyme (i.e., photolyase) and visible light exposure for activity. DNA photolyases are monomeric proteins (25-66 kDa in size) that consist of two cofactors, a light harvesting cofactor and a catalytic cofactor (Sancar 1994; Figure 1-4).

Unlike NER, which involves the coordination of multiple light energy (> 380 nm) to drive catalysis and directly reverse the monomeric bonds within each photoproduct. Light energy (> 380 nm) is captured by the antenna molecule of photolyases (e.g., MTHF, 8-HDF, FMN) and transferred to the catalytic cofactor FADH- that once excited may transfers energy to the pyrimidine dimer in the form of e- to split the dimer into two monomeric units (Sancar 1996). Although PER was first declared absent in mammalian cells by Cleaver in 1966, subsequent work by Setlow and Sutherland in 1974 reported a PER like activity in a limited subset of mammalian cells (Cleaver 1966, Sutherland 1974). It was not until further technological advances in DNA sequencing and protein structure identification that photolyases were identified in a wide range of organisms (Ley 1984; Kim *et al.*, 1993).

Studies have demonstrated that DNA repair processes such as NER and PER are critical in preventing photocarcinogenesis of the skin in both human and other animal models. The critical role of NER in human skin is demonstrated by rare autosomal-recessive NER-defective syndromes termed xeroderma pigmentosum (XP). Cleaver and Setlow first described the molecular basis of this disease in the late 1960s, providing evidence that cells from XP patients were unable to repair UV damage in their DNA (Cleaver *et al.*, 1968; Setlow *et al.*, 1969). The disease has since been linked to mutations in specific XP proteins (XPA, B, D, G) that result in increased sun sensitivity



Source: Sancar BS, and Sancar A, 2006

Figure 1-4: Proposed mechanisms for CPD and (6-4)PD photolyases.

Reaction mechanisms of the (A) pyrimidine dimer photolyase and (B) (6-4) photolyase. Both reaction mechanisms involve proton absorption (300-500 nm) by the photolyase through MTHF, transfer of the excitation energy to the flavin molecule, and donation of an electron to the photoproduct.

Table 1-1: Photolyase sequences that have been identified in multiple organisms by genomic resources. Genes encoding functional photolyase proteins have not been identified in placental mammals and are thought to have evolved into non-functional blue light photoreceptors involved in photoperiodism.

Organism	CPD Photolyase	6-4 Photolyase
<i>Escherichia coli</i>	+	-
<i>Saccharomyces cerevisiae</i>	+	-
<i>Arabidopsis thaliana</i>	+	+
<i>Drosophila melanogaster</i>	+	+
<i>Oryzias latipes</i>	+	+
<i>Danio rerio</i>	+	+
<i>Xiphophorus maculatus</i>	+	+
<i>Monodelphis domestica</i>	+	+
<i>Mus musculus</i>	-	-
<i>Homo sapiens</i>	-	-

(particularly UVB component) and a very high incidence of melanoma among other forms of cancer (Cleaver *et al.*, 1999). The association of a failure to repair direct DNA damage after UVB exposure in the skin of these patients and an increased incidence of early onset melanoma remains one of the strongest arguments for the role of UVB photoproducts in melanomagenesis.

Development of transgenic mice that contain either a CPD-photolyase from the marsupial *Potorous tridactylus*, a (6-4)PD photolyase from the plant *Arabidopsis thaliana*, or both have provided investigators the ability to selectively remove UVB-induced DNA lesions (Schul *et al.*, 2002). Although photoproducts are normally repaired by NER in the skin of mice, chronic exposure of wild type mice results in an abundance of tumor bearing animals. Photoreactivation within photolyase transgenic lines of similarly exposed mice results in a remarkable reduction of tumors, particularly in those possessing the CPD-photolyase gene. In contrast, (6-4)PD photolyase transgenic mice only show a slight reduction in UV induced tumorigenesis, indicating the more abundant CPD lesion contributes more significantly to the process of photocarcinogenesis than (6-4)PDs (Jans *et al.*, 2005).

Specific families of transcription factors (e.g., *AP-1*, *ATR*, *NF- κ B* and *P53*) and signaling proteins (MAPKs) become activated in human skin cells (keratinocytes) after UV exposure and regulate multiple cellular processes including DNA repair (Tyrell 1996). In the *AP-1* pathway, UVB exposure triggers a series of events that activate several MAP kinases, including stress activated protein kinases (SAPKs) such as *jun* kinases (JNKs) (Cooper *et al.*, 2007). Evidence suggests that UV may mimic growth factor/receptor interactions at the cell membrane and activate receptor kinases as well.

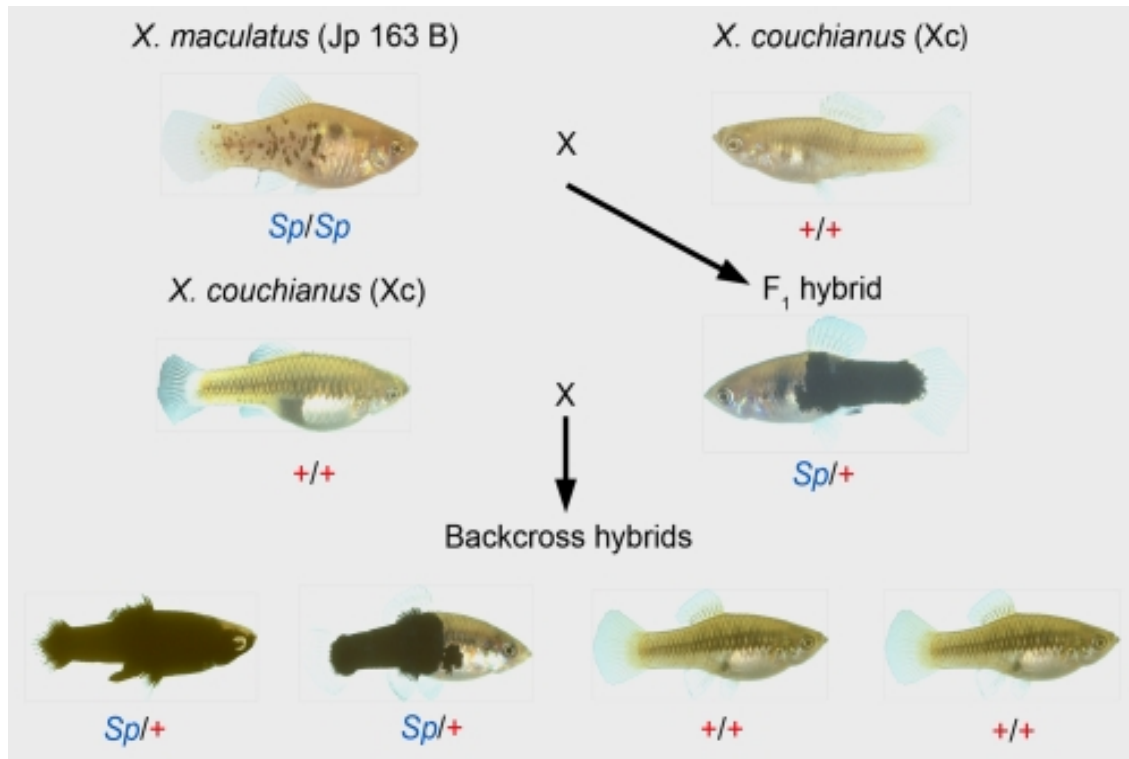
Membrane associated events such as *ras*-GTP binding also occur after UV exposure in human keratinocytes, leading to activation of a cascade of serine threonine protein kinases which regulate phosphorylation of *p53* and serve as a UV sensor to promote cell cycle arrest and prepare cells for DNA repair (Tibbetts *et al.*, 1999). Increased levels of such cellular signaling proteins (i.e., AP-1, *P53*, *MAPKs*) have been detected as early as 2 hrs after UV exposure and simulated sunlight (SS) exposure in human skin and can remain elevated from 8 to 24 hrs post exposure (Davenport *et al.*, 1999; López-Camarillo *et al.*, 2012). During this post exposure time period, multiple events such as DNA repair, epidermal remodeling, pigment production, and cell death can occur coincident with prolonged activation of specific sets of genes. It has been suggested the oxidative component of UVB (small relative to UVA), particularly singlet oxygen, may also be responsible for inducing the expression of many genes as well, including immune responsive and matrix remodeling genes (Maverakis *et al.*, 2010).

The complex interplay that exists between DNA photoproducts and UVB-induced transcriptional responses in the skin are still not fully understood, although both events are likely to contribute to melanomagenesis. Unlike other forms of skin cancer, the identification of UV photoproduct signature mutations in critical genes within human melanomas has been limited (Rass *et al.*, 2008). Additional genetic and molecular signaling components within the genetic background of an organism may be influenced by DNA damage and contribute to individual susceptibility to photocarcinogenesis (Jhappan *et al.*, 2003). Animal models such as *Xiphophorus* fish that are capable of PER and possess the vertebrate suite of NER proteins and cofactors are suitable for

approaching such questions since one may selectively remove UVB induced DNA damage in a subset of animals within an experimental design.

The *Xiphophorus* genus consists of 27 species of livebearing fish, which can be mated to produce fertile interspecies hybrids. Select *Xiphophorus* interspecies genetic hybrids have served as valuable tools for melanoma research since the 1920s (Gordon 1927; Kosswig 1928). A UVB inducible melanoma model has been described by crossing *X. maculatus* (Jp 163 B strain) with *X. couchianus* to produce F₁ interspecies hybrids that are then backcrossed to the parental *X. couchianus* (Nairn *et al.*, 2001; Mitchell *et al.*, 2006). During this crossing process, F₁ hybrids develop enhanced melanocytic pigmentation along the flanks of their body that in certain backcross progeny becomes even more enhanced (see Figure 1-5).

The origin of this pigmentation comes from the pigment cells of *X. maculatus* Jp 163 B that result in melanocytic spots along its body. Upon crossing with *X. couchianus*, these pigment cells become disregulated within F₁ hybrids and even further disregulated in select backcross progeny to produce a fish that may become almost totally black; however the melanocyte expansion does not develop in to melanoma unless these animals are exposed to UVB (6 days post birth) or MNU (6 weeks post birth; Kazianis *et al.* 2001a,b). Exposure of 6-day-old hyperpigmented backcross progeny fry to a daily dose of UVB for 5 days results in an increased incidence of melanoma within these animals at 6-8 months post exposure (Nairn *et al.*, 2001; Mitchell *et al.*, 2010). Tumors within these animals however can be reduced to background levels if they are exposed to fluorescent light, that promotes the removal of DNA photoproducts by PER, after exposure to UVB.



Source: Mitchell *et al.*, 2010

Figure 1-5: A *Xiphophorus* melanoma model hybridization scheme. F_1 hybrids are produced by mating the macromelanophore pigmented “spotted side” (Sp/Sp) *X. maculatus* strain Jp 163 B female to a *X. couchianus* male not carrying an Sp allele ($+/+$) and therefore not exhibiting any macromelanophore pigmentation. F_1 hybrids are then backcrossed to either male or female *X. couchianus* and produce backcross (BC_1) progeny of which ~50% exhibit the enhanced pigmentation phenotype ($Sp/+$) and ~50% exhibit the wild-type ($+/+$) pigmentation phenotype. Exposure of $Sp/+$ progeny to UVB while fry results in an increased onset of melanomas by adulthood.

This demonstrates that UVB induced DNA damage is one of the critical driving forces of melanomagenesis within these animals (Mitchell *et al.*, 2007).

NER, has also been studied within the skin of UVB exposed parental species, F₁ hybrids, and backcross hybrids of this crossing scheme (Mitchell *et al.*, 2001, 2004, 2009). DNA repair assays for both CPDs and (6-4)PDs revealed that both of these photoproducts are repaired with different efficiencies within the parental species *X. maculatus* Jp 163 B and *X. couchianus*. A greater repair rate was demonstrated in *X. couchianus* for both photoproducts relative to *X. maculatus*. In F₁ hybrids repair of both photoproducts are decreased compared to both parents, with repair of the (6-4)PD being remarkably reduced (Mitchell *et al.*, 2004). Within these studies, all fish were exposed to the same UVB dose that is used to generate tumors within backcross progeny (6.4 kJ). It was initially thought that this reduction in NER would be even more disregulated in backcross progeny, however, when the same experiments were conducted within these fish, a wide range of repair efficiencies of both photoproducts were found. When comparing these ranges within tumor bearing and non-tumor bearing fish no correlation was shown (Fernandez *et al.*, 2011). This work demonstrated that reduced global NER rates within backcross progeny is not linked directly to melanoma susceptibility after UVB exposure but likely was a result of chromosomal segregation into the BC₁ hybrids. Despite these results, repair of UVB induced DNA photoproducts remain a critical parameter within this melanoma model.

Although PER appears to be a major DNA repair mechanism involved in reducing melanomagenesis within these Xiphophorus models, little is known about the molecular events that occur during this process. Namely, how the removal of DNA photoproducts

by PER in the skin of *Xiphophorus* results in modulation of transcriptional responses that may influence the path to melanomagenesis. However, new methods for global assessment of gene expression using high throughput parallel sequencing coupled with RNAseq analysis of gene expression now make it possible to assess the effects of PER on the transcription response in UVB exposed fishes. Thus, to approach this question, we employed RNAseq technology to study global changes in gene expression that occur in the skin of select *Xiphophorus* fishes after UVB exposure, UVB and visible light exposure (PER conditions), and only visible light exposure. The animals chosen for this study were the two parental species *X. maculatus* Jp 163 B and *X. couchinaus* in addition to F₁ interspecies hybrids made by crossing these two parental species. Herein we present gene expression profiles and modulated expression shifts that correspond to each form of light exposure in the skin *X. maculatus* Jp 163 B.

CHAPTER 2

MATERIALS AND METHODS

Research animals:

Xiphophorus is a genus compassed of 26 species of live-bearing freshwater fishes. All *Xiphophorus* utilized in these studies were maintained in 20 gallon freshwater aquaria and fed commercial flake food (Tetramin) and/or newly hatched brine shrimp (*Artemia*) nauplii. The fish used in this study were all adult mature males and ranged in age from 7 to 12 months. Parental strains were obtained from the *Xiphophorus* Genetic Stock Center located at Texas State University-San Marcos, TX and have been maintained in a facility in Smithville, TX since 2000. *X. couchianus* was derived from the Huasteca canyon (1961; Nuevo Leon, Mexico). *X. maculatus* strain Jp 163 B was derived from a single field-inseminated mother in 1939 from the Rio Jamapa (Veracruz, Mexico) and offspring were split after about nine generations of inbreeding to generate the Jp 163 A and Jp 163 B strains. They are currently in their 90–100th generation of full-sibling inbreeding and thus are considered to be virtually 100% homozygous. The F₁ hybrids were obtained by natural or forced (artificial insemination) cross-breeding of the two parental species (i.e. *X. maculatus* Jp 163 B × *X. couchianus*; See figure 2-1).



X. maculatus Jp 163 B



X. couchianus



F₁ hybrid

Source: <http://www.xiphophorus.txstate.edu/>

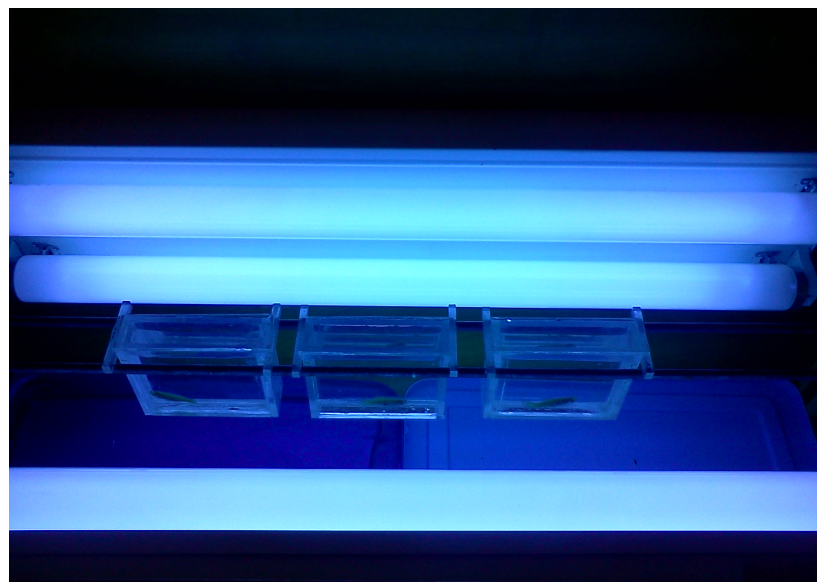
Figure 2-1: Images of *Xiphophorus* fish used within this study. The F₁ hybrid was generated by crossing the two parental species *X. maculatus* Jp 163 B and *X. couchianus*.

Light sources and exposures:

All light exposures occurred in a large wood box (Figure 2-2) that housed UV-transparent chambers that are suspended in the middle of the box such that three un-anesthetized, free-swimming fish (one per chamber) can be simultaneously exposed to UVB or photoreactivating light (PRL) from both sides. In order to reduce ‘edge’ effects (i.e., decreased or uneven exposure rates towards the ends of the box), we only placed 3 chambers into the center of the box at one time. To prevent unwanted white light effects (i.e., light-inducible photoenzymatic repair or PER) animals were kept in the dark 24 hours prior to exposure. For UVB, fish were exposed in 2 cm wide UV-transparent plastic chambers suspended between two banks of four unfiltered Philips TL01 UVB lamps mounted horizontally on each side of the exposure box about 10 cm from the center of the irradiation chamber. Fluence was measured on each side of the chamber filled with water using an IL-1400A Radiometer/Photometer coupled to a SEL 240/UVB detector containing a 280 nm Sharp Cutoff Filter (International Light, Newburyport, MA). The estimated dose rate was $12.2 \text{ J m}^{-2} \text{ s}^{-1}$; thus, exposure for 8 min 45 s yields a total dose of 6.4 kJ m^{-2} to both sides of the fish. For the UVB + PRL exposures, fish were exposed to 6.4 kJ m^{-2} UVB followed by exposure for 2 hrs to a bank of ‘‘Cool White’’ fluorescent lamps (General Electric, ~550 nm peak emission) filtered through Mylar 500D to exclude any wavelengths $<320 \text{ nm}$. Fish were also exposed only to PRL for 2 hrs without prior UVB exposure.

After UVB or PRL exposures fish were maintained in the dark to allow time for gene expression prior to being sacrificed for tissue dissection. This dark incubation was for 6 hrs after UVB exposure and for 4 hours after the PRL and UVB+PRL

exposures. Upon conclusion of dark incubation, fish were sacrificed using a lethal dose of anesthesia (MS-222) and multiple tissues (skin, brain, eyes, gill, liver, muscle) were dissected directly into RNAlater, frozen, and stored at -80°C . Skin from the side of each animal was dissected and stored separately so that DNA and RNA isolation could be independently isolated from the same animal.

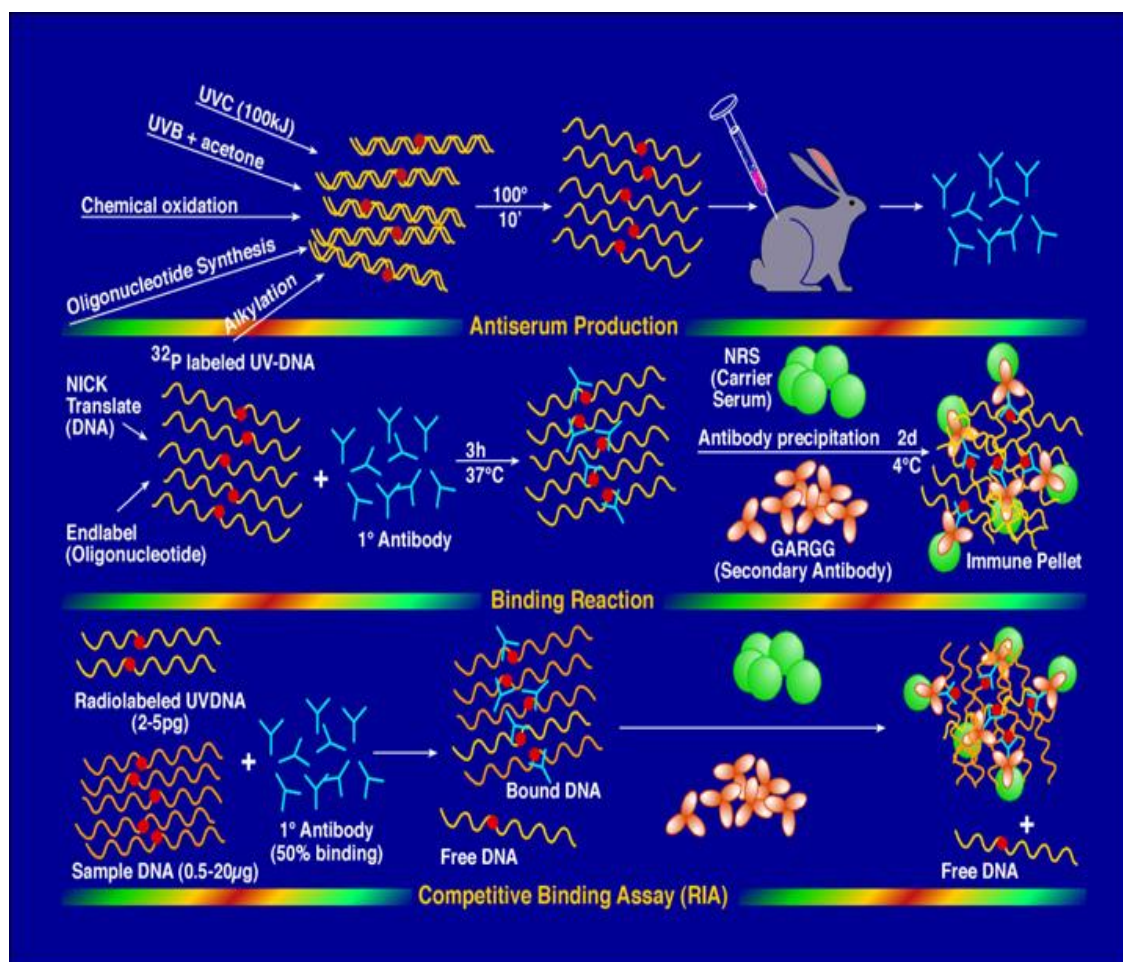


Source: Kevin Downs

Figure 2-2: Experimental light exposure set-up. Images of the exterior and interior of the exposure boxes used for UVB and PRL exposures. Three fish at a time were exposed to UVB light in 2 cm wide UV-transparent chambers suspended between two banks of four unfiltered Philips TL01 UVB lamps mounted horizontally on each side of the irradiation chamber at ~10 cm from the center of the irradiation chamber. The box used for PRL exposures used “Cool White” fluorescent lamps.

DNA isolation and radioimmunoassay:

DNA was isolated from skin samples using the Genomic-tip system (Qiagen). A Radioimmunoassay (RIA) was then used to measure UV photoproducts (CPDs and 6-4PDs) in purified DNA samples. An illustration of the RIA steps is presented in Figure 2-3. DNA samples were heat-denatured at 100°C for 10 min and then quenched on ice to prevent reannealing. Approximately 2-5 µg sample DNA was incubated with 5–10 pg of poly (deoxyadenosine):poly (deoxythymidine) (labeled to $>5 \times 10^8$ cpm/mg by nick translation with 32P-dTTP) in a total volume of 1 mL 10 mM Tris (pH 8.0), 1 mM EDTA, 150 mM NaCl and 0.2% gelatin (Sigma). Antiserum was added at a dilution that yielded optimal binding to labeled ligand. The dilution for the CPD primary antibody was 1/20,000 and the dilution for the (6-4)PDs was 1/200,000. After 3 hrs incubation at 37°C the immune pellet was precipitated for 2 days at 4°C with goat antirabbit immunoglobulin (Calbiochem) and normal rabbit serum (UTMDACC, Science Park/Veterinary Division, Bastrop, TX). The immune complex was centrifuged at ~3700 rpm for 45 min at 10°C and the supernatant discarded. The pellet was dissolved in 100 mL tissue solubilizer (NCS, Amersham), mixed with 6 mL ScintiSafe (Fisher) containing 0.1% glacial acetic acid and quantified using LSC (Packard Instruments). Sample inhibition was extrapolated through a standard (dose response) curve to determine the number of photoproducts in 10^6 bases. The standard consisted of double-stranded salmon testes DNA (Sigma) irradiated with increasing doses of UVC (254 nm) light. These details, as well as those concerning the specificities of the RIA, are described in Mitchell *et al.*, 2006. Once the data was obtained it was analyzed using an Excel spreadsheet and the results graphed with Sigma Plot software.



Source: Mitchell *et al.*, 2012

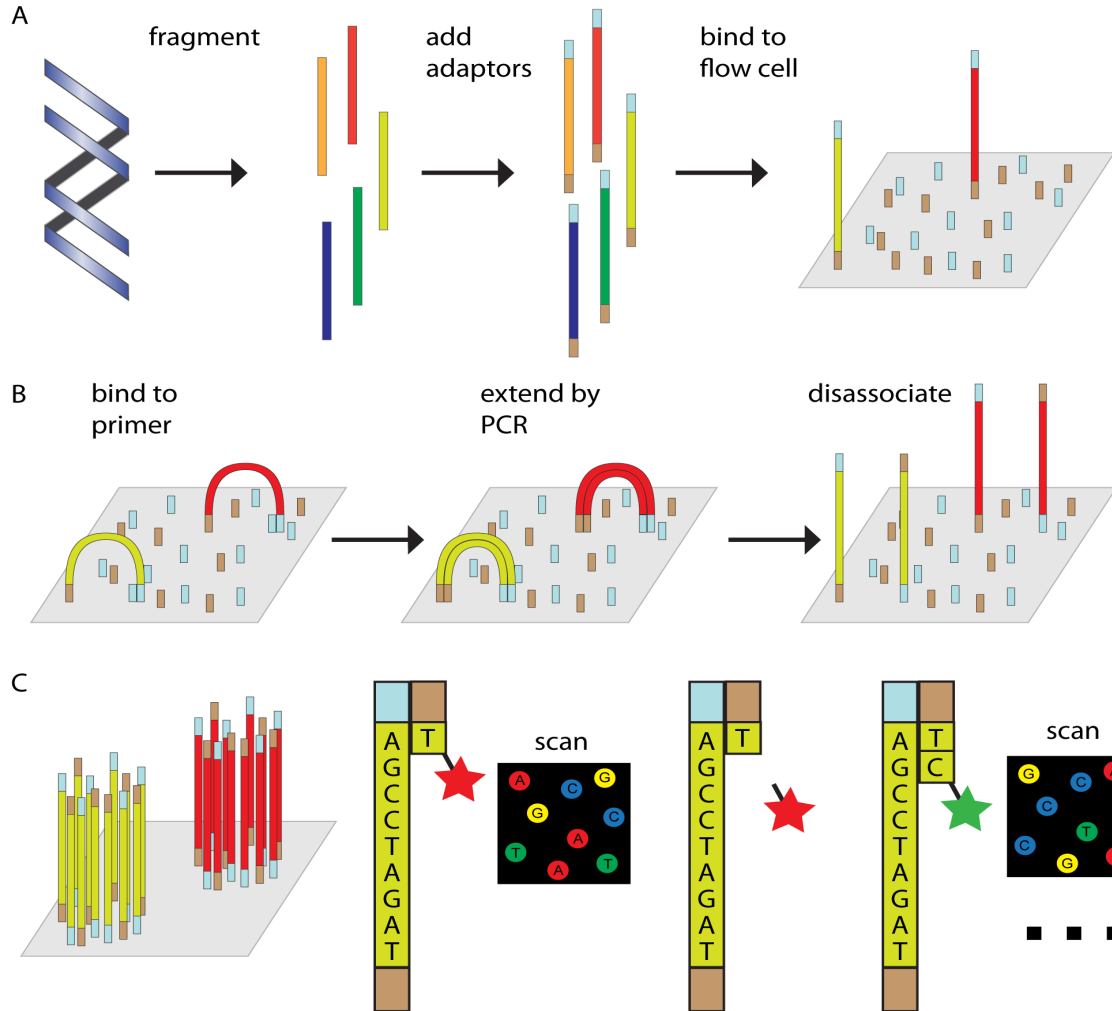
Figure 2-3: Diagram of radioimmunoassay (RIA) protocol for the quantification of CPDs and (6-4)PDs in DNA extracted from mammalian cells and tissues. For original antibody production, antisera were raised in rabbits against DNA that was irradiated with either 100 kJ/m² UVC (254 nm) light for (6-4)PDs or dissolved in 10% acetone and irradiated with UVB (311 nm) light under conditions that produce CPDs exclusively (Lamola, 1969).

RNA isolation:

For total RNA isolation, 1 mL TRIzol Reagent was added to each skin sample and homogenized using a handheld tissue disruptor. Following homogenization, samples were incubated at room temperature for 5 min followed by the addition of 0.2 mL chloroform. Tubes were vigorously shaken and allowed to incubate at room temperature for an additional 2 min followed by centrifugation at 12,000 x g for 15 min at 4°C. RNA was further purified using RNeasy mini RNA isolation kit (Qiagen, Valencia, CA). Any residual DNA was eliminated by performing column DNase digestion at 37°C (30 min). The integrity of RNA was assessed by gel electrophoresis (2% agarose in TAE running buffer) and the concentration was determined using a spectrophotometer (Nano Drop Technologies, Willmington, DE, USA).

RNA sequencing:

RNA isolated from the skin of *X. maculatus* Jp 163 B, *X. couchianus*, and an F₁ hybrid generated by crossing the two parental species was sequenced as 100 bp, paired end sequences (PE) using the Illumina High-Seq platform (Expression Analysis, Inc. Durham, NC). A total of four unique skin samples from each parental species and the F₁ hybrid were sequenced. These samples included UVB exposed skin (6.4 kJ m⁻² UVB), UVB + PRL exposed skin (6.4 kJ m⁻² UVB + 2 hrs PRL), PRL exposed skin (2 hrs PRL), and sham exposed skin (fish placed in irradiation chamber for duration of UVB exposure but no lights were turned on). An outline of the RNA sequencing process is depicted in Figure 2-4. Herein we present only the RNA sequencing data analysis for the *X. maculatus* Jp 163 B skin samples.



Source: Shen *et al.*, 2011

Figure 2-4: Overview of Illumina RNA sequencing. RNA is sheared into shorter fragments and then converted to cDNA. Unique adaptors are added to each of the cDNA molecule that allow them to attach to a lawn of primers on the flow cell. Fragments bend and bind to complimentary primers followed by being amplified by bridged PCR. The fragments dissociate and then another round of amplification is performed until dense clusters are formed. DNA polymerase and labeled nucleotides are then added and as bases are incorporated a laser is used to activate a fluorescent signal. Each cluster of cDNA is monitored by a computer and the color of each cluster is noted as each base in incorporated to generate a sequence consensus.

Short read filtration and assembly:

Reads were filtered and trimmed based on quality scores using a filtration algorithm that removed low scoring sections of each read and preserved the longest remaining fragment (Garcia *et al.*, 2012). Any reads with uncalled bases were rejected and a Phred quality score of 2 encoded in Fastq format as a 'B' was used as a special flag indicating that the results downstream of that position were untrustworthy. As a second step, portions downstream of 'B' quality scores were then removed. Finally, reads were broken apart anywhere the quality score value was 10 or below or where the average score of a position and its two neighbors was 20 or below. The largest remaining fragment of each read was kept (provided it was sufficiently long (i.e., 49 bp or more) and the rest were discarded. Reads that lost their mate pair were moved into a single-end file and the integrity of the remaining read-pairing information was maintained. VELVET was employed to guide the assembly using combined paired-end and singleton reads. K-mer sizes from 21 bases to 49 bases were used and compared assemblies produced from different K-mer sizes to identify the assembly with the longest N50 length.

Read alignment and analysis of differential expression:

The Bowtie short read alignment program was used to map each sample of short reads independently to a refined set of reference transcripts. The reads were aligned to a "reciprocal best hit" (RBHB) library that consisted of full cDNA libraries of 6 species (*Homo sapiens*, *Danio rerio*, *Gasterosteus aculeatus*, *Oryzias latipes*, *Tetraodon nigroviridis*, *Takifugu rubripes*) in addition to 580 manually annotated genes using Geneious software. A custom Perl script determined the number of reads mapped to each

contig from the alignment file. A second Perl script then compiled the number of reads per contig per sample into a tabular format. The first column of the data file contains the transcript identifier, and each subsequent column has the number of fragments mapped to that transcript in each sample. The DESeq package (ver 1.4.1, Bioconductor ver. 2.8, R ver. 2.13) was used to determine differential expression from the compiled tabular data. DESeq uses a model based on the negative binomial distribution to determine significance and was developed specifically to meet the challenges of working with short read RNA-Seq data. A significance level of $P < 0.01$ was used to select differentially expressed sequences. For determining gene expression within each exposed sample (UVB, UVB+PRL, PRL), fold changes were calculated based on the number of normalized reads present within the Sham skin sample relative to each exposed sample.

Quantitative real-time PCR:

Quantitative real-time PCR (qRT-PCR) was used to assess the relative gene expression levels of *JUN*, *JUN_2*, *JUNB*, *JUNB_2*, *FOS*, *FOSB*, and a CPD Photolyase in UVB, UVB + PRL, and PRL exposed skin of *X. maculatus* Jp 163 B. Primer sequences used in these reactions can be found in Table 2-1. The presence of two versions of *JUN* and *JUNB* in *Xiphophorus* required additional considerations for the design of these primers. In order to ensure amplification of only one version of each gene, the 3' end of these primers were designed within non-homologous nucleotide regions based on sequence alignments using Geneious software. Primers that amplified both copies these genes were also designed as a control. Total RNA was extracted using TRIZOL (Invitrogen) and first strand cDNA was synthesized with Multiscribe Reverse

Transcriptase (Applied Biosystems). Real-time PCR reactions were performed with a 7500 Fast Real-Time PCR System using the Fast SYBR Green Master Mix detection method (Applied Biosystems). For each assay a total of 100 ng cDNA was used in triplicate.

To normalize target gene expression for differences in cDNA input, cDNA was diluted an additional 1/500 for measuring 18S rRNA levels. Diluted cDNAs (8 μ L aliquots) were added to the wells of a 96-well plate with 10 μ L of Fast SYBR Green Master Mix and 0.5 μ M of each primer pair. For quantification of PCR results cycle threshold (C_T) values were determined for each reaction. A standard curve was constructed from data derived using a dilution series of whole fish cDNA expected to possess significantly high gene expression. The standard curve allowed assessment of the relationship between the quantity of starting material and the C_T values as an indicator of the primer efficiency for gene amplification. Relative gene expression was determined using the comparative ΔC_T method by comparing the gene of interest C_T values with the 18S values. For each assay, gene expression in unexposed SHAM skin was chosen for calculating the fold change in expression.

Table 2-1: Primers used for gene expression analysis by quantitative real-time PCR. The two versions of *JUN* (*JUNA* and *JUNA_2*) and *JUNB* (*JUNB* and *JUNB_2* in *Xiphophorus* required additional considerations for the design of these primers. In order to ensure amplification of only one version of each gene, the 3' end of these primers were designed within non-homologous nucleotide regions based on sequence alignments using Geneious software. Primers that amplified both copies these genes (*JUNA*** and *JUNB****) were also designed and tested as a control.

Gene ID	Forward Sequence (5' - 3')	Reverse Sequence (5' - 3')
JUNA**	TCCCCGATCGACATGGAGAACCA	CGGTCCTCATGCGCTTCCTCT
JUNA	ACTGTTTATAACAACACCCCGGCCA	CGGGTTGAACGTGTTCAAGTCCTC
JUNA_2	AACCTGGCCGGTTTTAGCCGAA	GGTAACTTGTAGGCGGGTGCCT
JUNB**	GACTCGTTTCTCTCTGCTTATGGCCA	TTTAGCAGCTTGTAGTCTGTCAGGGC
JUNB	CTCCGATTCATATCGGAACCCGAGCT	CCGCCGGGTAGAAATCACTGTCT
JUNB_2	TCGGCTTACGGCCACTCAGAT	TCAGGTTGCGATAGGGCTCTGTC
FOS	CCATCAGGATCTTATCCAGC	ATTGAGGAACAAGCAGGC
FOSB	CCATAGAGTCCCAGTACCTATCCTCCG	GCACAAATGAACCTGGCATCTCACC
Photolyase	GTGGCTGAACGACGTCAAAAAGAAGC	AGCGTAATGTCTCAGTGTGGACAGC

CHAPTER 3

DETERMINATION OF UVB-INDUCED PHOTOPRODUCT FORMATION AND LIGHT INDUCED MODULATION OF GENE EXPRESSION IN *XIPHOPHORUS* SKIN.

When skin is exposed to UVB radiation a portion of the energy is directly absorbed by cellular components such as DNA. When this occurs, adjacent pyrimidine bases within double stranded DNA may dimerize by formation of high-energy covalent bonds leading to structures referred to as DNA photoproducts. The two major photoproducts that arise in DNA after UVB exposure are cyclobutane pyrimidine dimers (CPDs) and the pyrimidine(6-4)pyrimidinone dimer [(6-4)PD)] between adjacent bases. Accumulation of these photoproducts in DNA results in the formation bulky adducts that can alter or block normal DNA replication and transcription. UVB exposure may also generate reactive oxygen species (ROS) in the presence of photosensitizers commonly found within skin such as melanin and other pigment granules. The generation of ROS within cells can result in both direct and indirect DNA damage through the formation of monomeric photoproducts (photohydrates), oxidation products, deaminated products, single strand breaks, and DNA-protein crosslinks.

The two major pathways involved in the repair of DNA photoproducts are nucleotide excision repair (NER) and photoenzymatic repair (PER). Unlike NER, that is present in all organisms and is carried out by a large number of proteins, PER is largely absent in mammals and only requires a single protein (photolyase). Both NER and PER

activity have been demonstrated in the skin of several different species of *Xiphophorus* and PER repairs photoproducts orders of magnitude faster than does NER. PER has also been shown to play a critical role in preventing UVB induced melanoma in select interspecies hybrids of *Xiphophorus* fish. These experiments highlight the importance of DNA damage and repair in the initiation of melanoma within these animals. Currently, little is known about the transcriptional responses that occur in *Xiphophorus* skin after UVB and/or photoreactivating light (PRL) exposure. It seems likely that specific regulatory signaling pathways may become activated after UVB exposure and then are subsequently modulated by PRL exposure.

To begin to assess response of signaling pathways to UVB and/or PRL we exposed fish from two parental species (*X. maculatus* Jp 163 B and *X. couchianus*), and an F₁ interspecies hybrid produced by crossing these parental lines, to UVB alone, UVB + PRL, or only to PRL. The fish skin was dissected and both DNA and RNA and independently isolated from each animal. DNA damage in skin of all three fish types for UVB and UVB + PRL exposure was quantified by a radioimmunoassays (RIA) specific for CPDs or (6-4)PDs. To identify transcriptional responses that occur in the skin of these animals after light exposure, next generation RNA sequencing was employed. After filtering and mapping the short RNA sequence reads to a reference transcriptome assembly (20,147 total), the mapping efficiency for each transcript was determined as a measure of gene expression. In this manner, *X. maculatus* Jp 163 B skin was assessed for modulated gene expression after varied light exposures (UVB, UVB+PRL, or PRL). DESeq software was employed to compare the number of reads within each light exposed sample to those in the SHAM treated samples with applied confidence scores (P value).

Results:**A.) Induction of CPDs and (6-4)PDs in the skin of *Xiphophorus* fishes.**

To determine the number of UVB-induced photoproducts in the skin of *X. maculatus* Jp 163 B, *X. couchianus*, and an F₁ hybrid made by crossing the two parental species, a radioimmunoassay (RIA) specific for CPDs and (6-4)PDs was employed (Mitchell *et al.*, 2012). In this study we determined the number of CPDs and (6-4)PDs in skin that was exposed to 6.4 kJ/m² UVB, or to the same dose of UVB followed by photoreactivating light (PRL) comprised of 2 hours exposure to fluorescent light (i.e., PER conditions). CPDs were induced at a higher frequency in all UVB exposed skin samples, relative to the (6-4)PD. UVB exposed *X. couchianus* skin exhibited a significantly higher number of both CPDs and (6-4)PDs (> 3 fold), compared to *X. maculatus* Jp 163 B and the F₁ hybrid at the same doses. Fish that were exposed to PRL after UVB showed significantly less photoproducts (~60-80%), indicating functional PER for both CPDs and (6-4)PDs in exposed skin. The only exception was the F₁ hybrid that showed only a small reduction (~10%) in the number of (6-4)PDs upon exposure to PRL after UVB compared to both *X. maculatus* Jp 163 B and *X. couchianus*. The number of (6-4)PDs induced in UVB exposed F₁ hybrid skin however was nearly equivalent to unexposed SHAM skin (9.5 vs 7.4).

Table 3-1: Radioimmunoassay (RIA) detection of CPDs in *Xiphophorus* skin. CPDs were quantified in the skin of *X. maculatus* Jp 163 B, *X. couchianus*, and an F₁ hybrids made by crossing these two parental species after UVB exposure (6.4 kJ/m² UVB) or UVB + PRL exposure (6.4 kJ/m² UVB + 2 hours photoreactivating light). There were a total of 3 biological replicates (DNA isolated from the skin from 3 different fish) for each species/exposure group and 2 technical repeats for determining \pm standard deviation values.

Animal	Exposure	CPDs/MB
<i>X. maculatus</i> Jp 163 B	Sham	9.5 \pm 1.9
<i>X. maculatus</i> Jp 163 B	UVB	63.1 \pm 7.9
<i>X. maculatus</i> Jp 163 B	UVB + PRL	13.2 \pm 6.4
<i>X. couchniaus</i>	Sham	7.6 \pm 2.0
<i>X. couchianus</i>	UVB	173.5 \pm 26.2
<i>X. couchianus</i>	UVB + PRL	40.6 \pm 17.8
F ₁ Hybrid	Sham	9.6 \pm 3.0
F ₁ Hybrid	UVB	46.7 \pm 18.3
F ₁ Hybrid	UVB + PRL	18.2 \pm 7.2

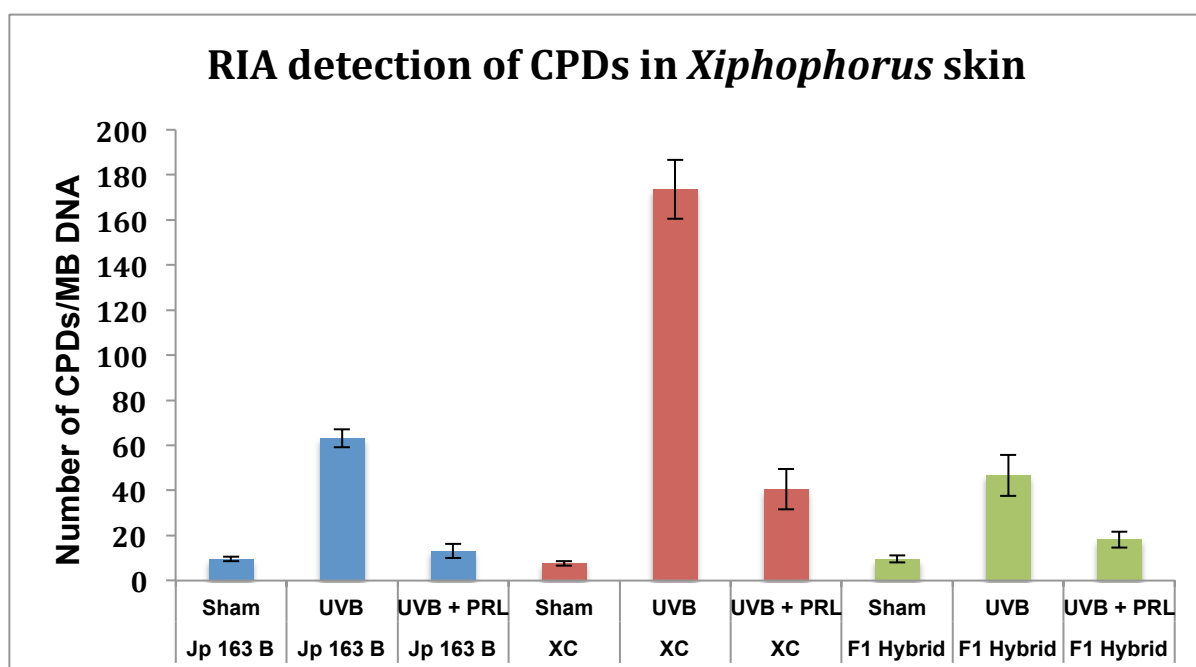


Figure 3-1: Radioimmunoassay (RIA) detection of CPDs in *Xiphophorus* skin. CPDs were quantified in the skin of *X. couchianus* (XC), *X. maculatus* (Jp 163 B), and an F₁ hybrids made by crossing these two parental species after UVB exposure (6.4 kJ/m² UVB) or UVB + PRL exposure (6.4 kJ/m² UVB + 2 hours photoreactivating light). There were a total of 3 biological replicates (DNA isolated from the skin from 3 different fish) for each species/exposure group and 2 technical repeats for determining \pm standard deviation values.

Table 3-2: Radioimmunoassay (RIA) detection of (6-4)PDs in *Xiphophorus* skin. (6-4)PDs were quantified in the skin of *X. maculatus* Jp 163 B, *X. couchianus*, and an F₁ hybrids made by crossing these two parental species after UVB exposure (6.4 kJ/m² UVB) or UVB + PRL exposure (6.4 kJ/m² UVB + 2 hours photoreactivating light). There were a total of 3 biological replicates (DNA isolated from the skin from 3 different fish) for each species/exposure group and 2 technical repeats for determining \pm standard deviation values.

Animal	Exposure	(6-4)PDs/MB
<i>X. maculatus</i> Jp 163 B	Sham	0.9 \pm 0.4
<i>X. maculatus</i> Jp 163 B	UVB	5.1 \pm 3.0
<i>X. maculatus</i> Jp 163 B	UVB + PRL	1.4 \pm 0.4
<i>X. couchniaus</i>	Sham	5.8 \pm 1.1
<i>X. couchniaus</i>	UVB	47.4 \pm 14.5
<i>X. couchniaus</i>	UVB + PRL	14.1 \pm 2.1
F ₁ Hybrid	Sham	7.4 \pm 1.3
F ₁ Hybrid	UVB	9.5 \pm 0.7
F ₁ Hybrid	UVB + PRL	8.4 \pm 3.0

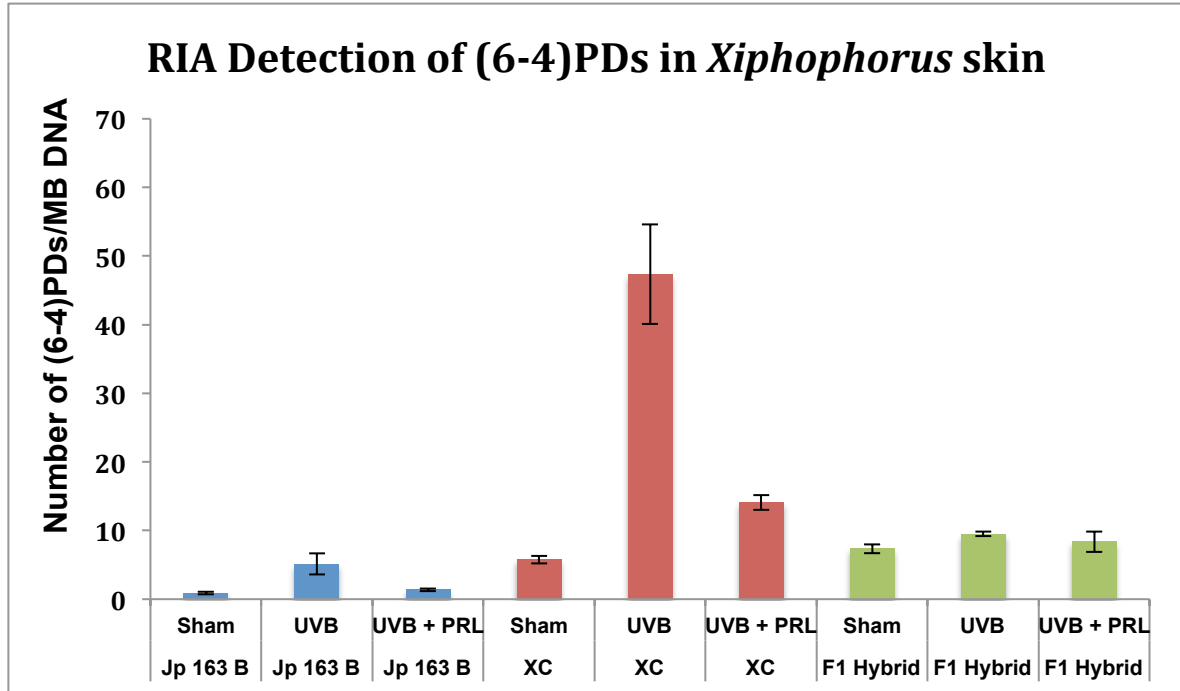


Figure 3-2: Radioimmunoassay (RIA) detection of (6-4)PDs in *Xiphophorus* skin. (6-4)PDs were quantified in the skin of *X. maculatus* Jp 163 B, *X. couchianus*, and an F₁ hybrids made by crossing these two parental species after UVB exposure (6.4 kJ/m² UVB) or UVB + PRL exposure (6.4 kJ/m² UVB + 2 hours photoreactivating light). There were a total of 3 biological replicates (DNA isolated from the skin from 3 different fish) for each species/exposure group and 2 technical repeats for determining ± standard deviation values.

B.) Identification of differential gene expression in the skin of *X. maculatus* Jp 163 B after UVB, UVB + PRL and PRL exposure.

To determine differential gene expression between SHAM-exposed skin and UVB (6.4 kJ/m²), UVB + PRL (6.4 kJ/m² UVB + 2 hrs PRL), or PRL (2 hrs PRL) exposed skin from *X. maculatus* Jp 163 B, Illumina high throughput RNA sequencing was employed to obtain short read (100 bp paired end) RNA sequence data. After appropriate filtration and processing the short read data was analyzed using the DESeq software package (R-package) to test for differential read count patterns within pair wise compared sequencing data. Count variance was estimated across conditions (SHAM vs. each exposed sample), based on the null assumption that genes behave the same across conditions. These values were determined to be 0.979 (UVB), 0.919 (UVB+PRL), and 0.882 (PRL). The PRL exposed skin sample had the highest size variance and was the least correlated sample in terms of average gene expression.

To determine differential gene expression, log-fold changes (log₂FC) and p-values were calculated for each transcript within SHAM skin and UVB, UVB+PRL, or PRL exposed skin. Genes were considered to have significantly different expression if the log₂FC had a P val < 0.01. Plots illustrating the number of significantly expressed genes within each sample are shown in Figures 3-3, 3-4, and 3-5. The greatest number of significant expression fold changes is observed for the PRL exposed skin sample (4,027) followed by UVB + PRL exposed skin (2,099). The UVB exposed skin had the smallest number of significant expression fold changes (912).

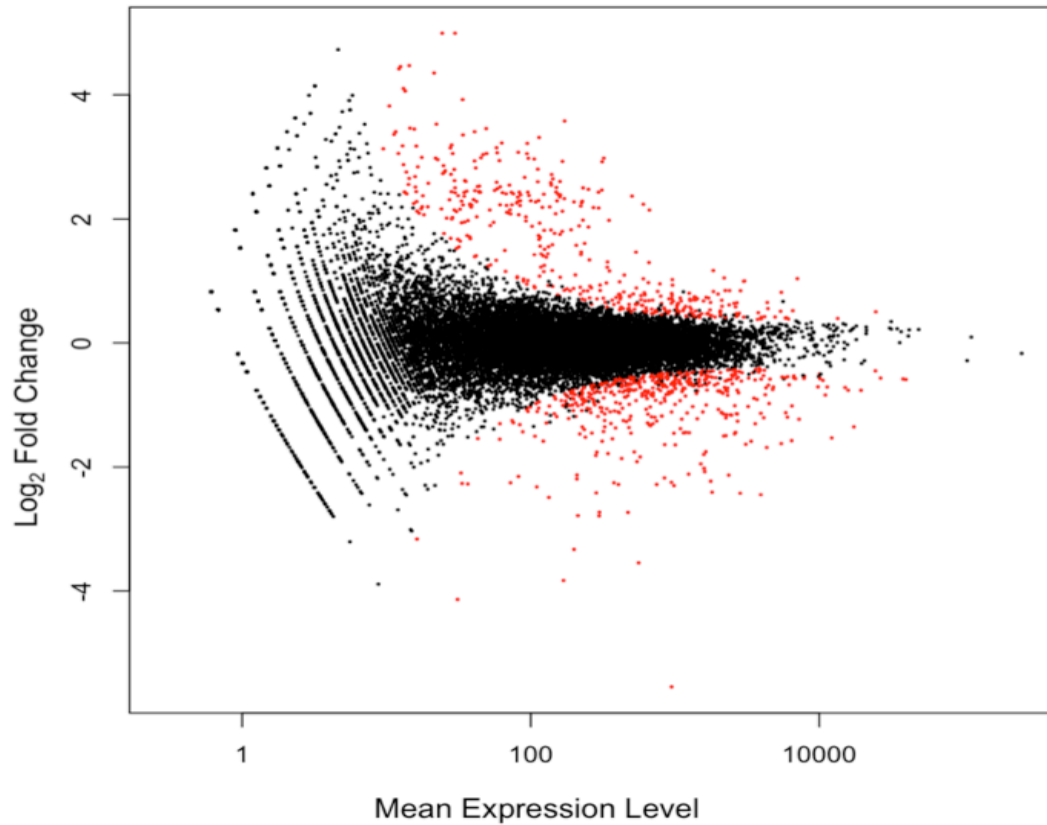


Figure 3-3: Transcript expression differences in UVB exposed (6.4 kJ/m^2 UVB) vs. unexposed skin from *X. maculatus* Jp 163 B determined by DESeq analysis. Each point represents the mean expression level plotted against the \log_2 fold change for that given transcript. Black points are those that are not statistically significant, and red points are significant at $P < 0.01$. A total of 20,147 assembled transcripts were used for this analysis and 912 are determined to have significant fold change values.

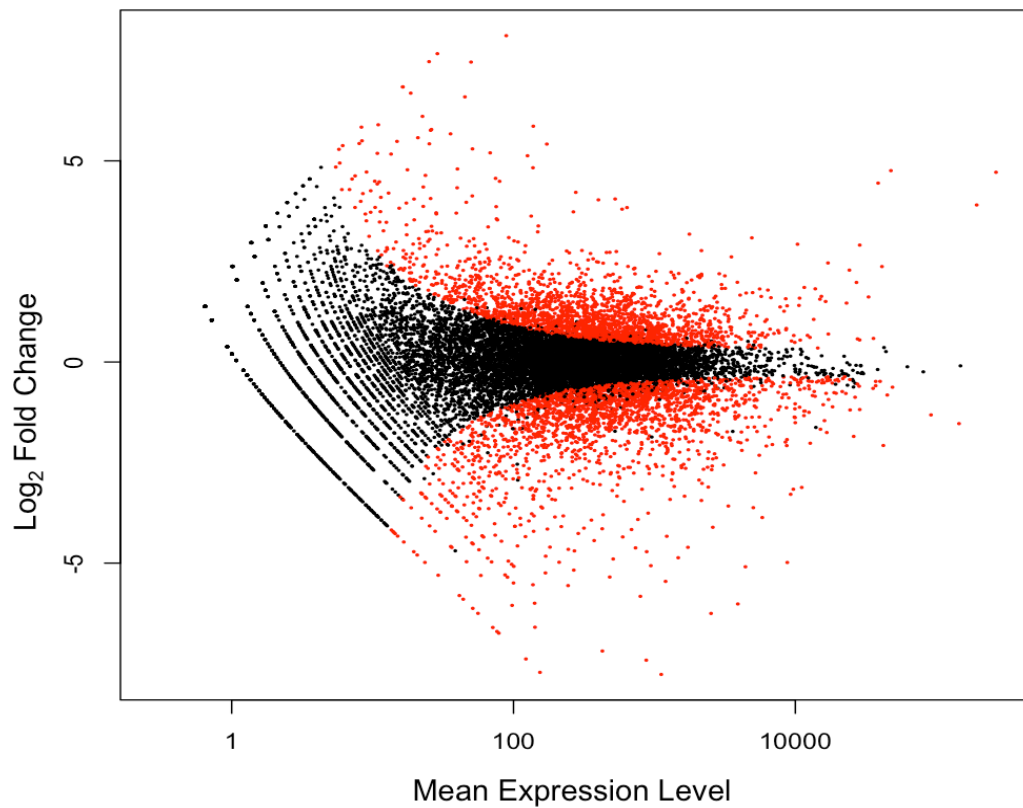


Figure 3-4: Transcript expression differences in UVB + PRL exposed (6.4 kJ/m^2 UVB + 2 hrs PRL) vs. unexposed skin from *X. maculatus* Jp 163 B determined by DESeq analysis. Each point represents the mean expression level plotted against the \log_2 fold change for that given transcript. Black points are those that are not statistically significant and red points are significant at $P < 0.01$. A total of 20,147 assembled transcripts were used for this analysis and 2,099 are determined to have significant fold change values.

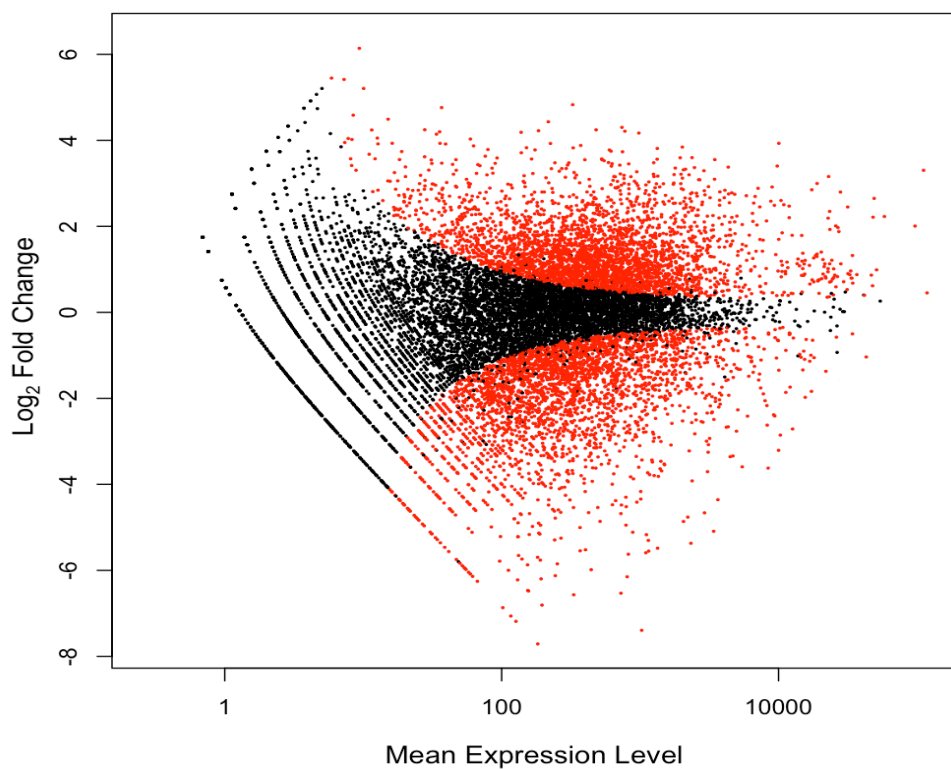


Figure 3-5: Transcript expression differences in PRL exposed (2 hrs PRL) vs. unexposed skin from *X. maculatus* Jp 163 B determined by DESeq analysis. Each point represents the mean expression level plotted against the log₂ fold change for that given transcript. Black points are those that are not statistically significant, and red points are significant at $P < 0.01$. A total of 20,147 assembled transcripts were used for this analysis and 4,027 are determined to have significant fold change values.

C.) Up-regulated and down-regulated genes in the skin of *X. maculatus* Jp 163 B after UVB, UVB + PRL and PRL exposure.

Genes that were suggested to have significant fold changes in expression within the UVB, UVB + PRL, or PRL samples were grouped depending on whether they were considered up-regulated or down-regulated after each light exposure (compared to SHAM skin). Additional \log_2 FC cutoffs (2, 3, and 4 Log₂FCs) were applied to identify the range at which the greatest amount of differential expression occurs (Tables 3-3 and 3-4). In both the UVB and UVB + PRL exposed skin samples, there were more down-regulated genes (493 in UVB and 866 in UVB + PRL) than up-regulated genes (419 in UVB and 1,231 in UVB + PRL). In contrast, the PRL skin sample had a much greater number up-regulated genes (2,776) compared to down-regulated genes (1,551). The greatest levels of gene expression fold changes (both up-regulated and down-regulated) occurred below a \log_2 FC of less than 2 for all three samples. For genes that were significantly up-regulated, approximately 68% in the UVB exposed sample, 88% in the UVB + PRL exposed sample, and 86% in the PRL exposed sample exhibit a \log_2 FCs less than 2. For genes that were significantly down-regulated, approximately 93% in the UVB exposed sample, 82% in the UVB + PRL exposed sample, and 76% in the PRL exposed sample has \log_2 FCs less than 2.

Table 3-3: Separation of significant up-regulated transcripts by fold change values. Comparison of up-regulated transcripts in *X. maculatus* Jp 163 B skin after UVB exposure (6.4 kJ/m² UVB), UVB + PRL exposure (6.4 kJ/m² UVB + 2 hrs PRL), or PRL exposure (2 hrs PRL). Fold changes were determined by DESeq analysis comparing normalized read counts present within each exposed skin sample vs. SHAM exposed skin. Log₂ fold change cutoffs were applied in order to generate separate lists of genes based on expression values. Transcripts that possessed less than 50 mapped reads were excluded from this list.

Transcript Fold Change Values	UVB	UVB + PRL	PRL
Total number	419	866	2776
Log ₂ Fold Change > 2	131	98	383
Log ₂ Fold Change > 3	35	10	97
Log ₂ Fold Change > 4	4	4	9

Table 3-4: Separation of significant down-regulated transcripts by fold change values. Comparison of down-regulated genes in *X. maculatus* Jp 163 B skin after UVB exposure (6.4 kJ/m² UVB), UVB + PRL exposure (6.4 kJ/m² UVB + 2 hrs PRL), or PRL exposure (2 hrs PRL). Fold changes were determined by DESeq analysis by comparing read counts present within each exposed skin sample vs. SHAM exposed skin. Log₂ fold change cutoffs were applied in order to generate separate lists of genes based on expression values. Genes that possessed less than 50 mapped reads were excluded from this list.

Expression Fold Change	UVB	UVB + PRL	PRL
Total Number	493	1231	1551
Fold Change > 4	34	229	366
Fold Change > 6	6	41	99
Fold Change > 8	2	5	21

D.) Comparison of differential gene expression in the skin of *X. maculatus* Jp 163 B after UVB, UVB + PRL and PRL exposure.

In order to identify genes within *X. maculatus* Jp 163 B that possessed similar modulation of gene expression after UVB, UVB + PRL, and PRL, up-regulated and down-regulated genes were compared across all three samples. Venn diagrams illustrating these results can be found in figures 3-6 and 3-7. The highest number of common up-regulated and down-regulated genes were observed between the UVB + PRL and PRL exposed skin samples. Out of the total 866 up-regulated genes in the UVB + PRL sample and 2,776 up-regulated genes in the PRL sample, 167 were common between the two. When comparing the total 419 up-regulated genes in the UVB exposed skin sample to those in the UVB + PRL, and PRL samples, only 25 were common to the UVB + PRL exposed sample and 58 to the PRL sample. Of the total 1,231 down-regulated genes in the UVB + PRL sample and 1551 down-regulated genes in the PRL sample 180 were common. Comparison of the total 493 down-regulated genes in the UVB exposed skin sample to those in the UVB + PRL and PRL samples revealed 113 in common with the UVB + PRL exposed sample and 85 for the PRL sample. A subset of genes in both the up-regulated and down-regulated lists for all samples also showed common expression. There were 125 genes that were significantly up-regulated and 8 that were significantly down-regulated in all three light exposed samples.

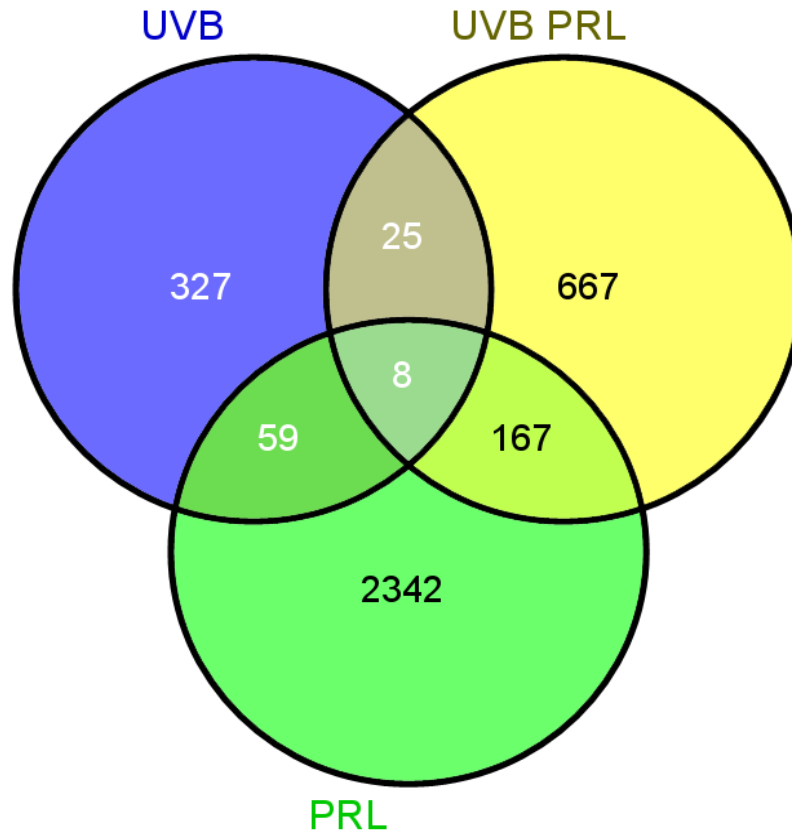


Figure 3-6: Venn diagram comparison of significant up-regulated genes (\log_2 fold change with, $P < 0.01$) in *X. maculatus* Jp 163 B skin after UVB exposure (6.4 kJ/m^2 UVB), UVB + PRL exposure (6.4 kJ/m^2 UVB + 2 hrs PRL), or PRL exposure (2 hrs PRL).

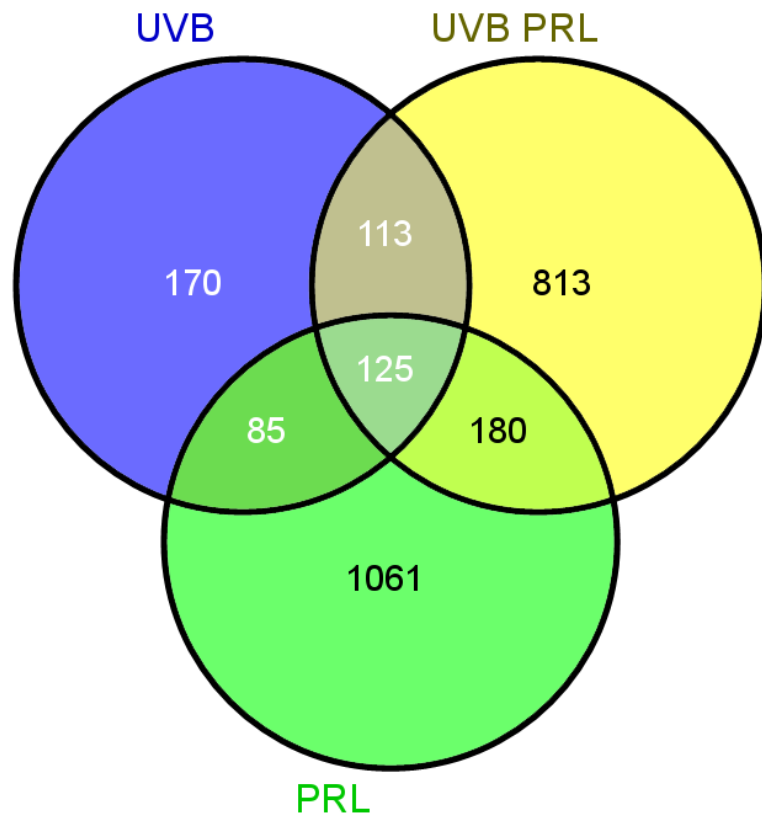


Figure 3-7: Venn diagram comparison of significant down-regulated genes (\log_2 fold change with $P < 0.01$) in *X. maculatus* Jp 163 B skin after UVB exposure (6.4 kJ/m^2 UVB), UVB + PRL exposure (6.4 kJ/m^2 UVB + 2 hrs PRL), or PRL exposure (2 hrs PRL).

Discussion:

In this study, levels of CPDs and (6-4)PDs were quantitatively determined in the skin of *X. maculatus* Jp 163 B, *X. couchianus*, and an F₁ hybrid made by crossing these two parental species after both UVB exposure (6.4 kJ/m²) and UVB + PRL exposure (6.4 kJ UVB and 2 hrs fluorescent light, PRL). A greater proportion of CPDs relative to (6-4)PDs were detected in the skin of all three fish types after UVB exposure, consistent with the induction rate observed in most vertebrates. Of the three *Xiphophorus* fish type used (e.g., two parental and the F₁ hybrid), *X. couchianus* skin showed the highest induction of both photoproducts after UVB exposure. This is likely due to the absence of heavy melanin pigmentation within the skin of these animals compared to *X. maculatus* JP 163 B and the F₁ hybrid.

Both *X. maculatus* Jp 163 B and the F₁ interspecies hybrid possess melanized skin (greatly enhanced in the F₁ hybrid). Melanin is known to strongly absorb UVB energy and serve as a shield for DNA in the skin by forming layers around the nuclear envelope. This may explain why the macromelanophore spotted side “Sp” *X. maculatus* Jp 163 B had fewer photoproducts present within its skin with an even further reduction observed in the hyperpigmented F₁ hybrid compared to *X. couchinaus*. Although melanin may possess the ability to protect DNA from direct UVB damage, it also must transfer absorbed energy in the form of heat or electron transfer to other cellular components within a short time period. This raises an interesting question as to how UVB energy, absorbed by melanized skin, is dissipated within these animals. One might argue that although direct DNA damage is being prevented within *X. maculatus* Jp 163 B and the F₁ hybrid, the increased melanin content may also cause the formation of reactive oxygen

species (ROS) due to electron spin off of the absorbed energy that cannot be quickly dissipated directly as heat.

Previously it was shown that the F₁ interspecies hybrids made by crossing the parental species *X. maculatus* Jp 163 B and *X. couchianus* had a reduced nucleotide excision repair (NER) rate of CPDs and a much more dramatic reduction in dark repair of (6-4)PDs (Mitchell *et al.*, 2003). Although the results presented here are not indicative of this phenomenon due to the single time point analyzed, it is still noted that even though there was a decreased induction of photoproducts within this animal it still possesses a decreased excision repair capacity for UVB photoproducts. Previous work using cultured human skin fibroblasts (NHSEFs) has investigated the effects of melanin content on excision repair of both CPDs and (6-4)PDs (Wang *et al.*, 2010). It was found that addition of melanin to UVC irradiated DNA in solution resulted in a dramatic decrease in excision repair sensitivity. The removal of melanin from these same DNA samples however dramatically restored the excision repair sensitivity. Although these results are rather far from what occurs *in vivo*, it is possible that a similar mechanism is occurs within the hyperpigmented skin of the F₁ hybrids.

Exposure of a subset of fish to PRL for 2 hrs after UVB exposure resulted in a significant decrease in both types of photoproducts to nearly background levels. This is consistent with results in Mitchel et al. (1993) that found a peak reduction of photoproducts occurs after 2 hrs of visible light exposure. It is largely for this reason the 2 hrs exposure time point was chosen for this study. Most studies examining photoreactivation in animals largely focus on the repair of CPDs since it is the major mutagenic lesion. Unfortunately, this has contributed to a lack of knowledge surrounding

the presence and efficiency of (6-4) photolyases within vertebrates. Based on our results, it is evident that *Xiphophorus* fish possess both a CPD photolyase and (6-4) photolyase activities that repair these lesions with similar efficiencies.

In order to determine the molecular genetic transcriptional responses occurring within the skin of these same animals after exposure to UVB, UVB + PRL, or PRL alone, we employed RNAseq technology. Unlike microarray analysis, RNAseq is not confined to a reduced cDNA library containing only a subset of well-defined genes. Results are presented from RNAseq data analyses from the skin of *X. maculatus* Jp 163 B after UVB, UVB + PRL, and PRL exposure. After the initial short read filtration, RNAseq reads were aligned to a “reciprocal best hit” (RBHB) database consisting of transcripts matching cDNA annotations from 6 reference species (*Homo sapiens*, *Danio rerio*, *Gasterosteus aculeatus*, *Oryzias latipes*, *Tetraodon nigroviridis*, *Takifugu rubripes*). This RBHB database also represented 580 manually annotated genes to form our reference transcriptome for read mapping. DESeq software was then used to determine genes within each sample (UVB, UVB + PRL, and PRL exposed) that had significant (P val < 0.01) log₂ fold changes in expression values (log₂FCs) compared to the SHAM treated skin. The results indicate a higher amount of differential gene expression occurred within the PRL and UVB + PRL exposed samples compared to the UVB exposed ones.

The PRL sample had the highest number of genes showing treatment altered, changes in gene expression (both up- and down-regulated), compared to the UVB and UVB + PRL exposed samples. Both the UVB and UVB + PRL exposures had a larger number of genes that were significantly down-regulated (nearly twice as many for the

UVB + PRL) compared to the PRL sample. In order to further assess gene expression changes in these data, multiple log₂FCs were applied to each data set (up- or down-regulated genes). Comparisons between the genes that were up-regulated or down-regulated within each sample was also completed in order to identify genes that may have similar or antagonistic expression after UVB and/or PRL exposure. Comparison of all of the up- genes and down-regulated genes across all samples revealed a higher number of genes in common between the UVB + PRL and PRL exposed samples. It is possible the higher number of shared genes in the UVB + PRL and PRL samples are genes modulated by the longer wavelength light after UVB exposure. On the other hand, genes that were up-regulated or down-regulated within the UVB Genes that were similarly expressed in all three samples were also identified, with a much larger set present within the down-regulated genes (125 compared to only 8 in up-regulated). It is possible that several of these genes are commonly expressed in all samples are light responsive regardless of spectra or are part of a generalized stress response that occurs after light exposure.

CHAPTER 4

IDENTIFICATION OF BIOLOGICAL PATHWAYS MODULATED BY UVB AND/OR PRL EXPOSURE IN *X. MACULATUS* JP 163 B SKIN.

Previous work with various animal models and human tissue cell culture has highlighted molecular pathways modulated by UVB light exposure in the skin. There are two major molecular responses that occur after UVB exposure in mammalian skin. The first is the DNA damage response (DNA repair, cell cycle arrest, apoptosis) and the second is the activation of cell surface receptors (growth factor, cytokine) and signal transduction molecules (MAPKs). The DNA damage response is largely determined by DNA damage signaling proteins (e.g. TP53, CDKs, ATM, ATR, RADs, CHEKs) that promote cell cycle arrest and can directly stimulate the expression and activity of DNA repair proteins (Friedberg *et al.*, 2003). The relative crosstalk that occurs between multiple biological pathways that are simultaneously activated in the skin after UVB exposure is still not fully understood and may involve additional molecular signaling events not yet described.

Although our fascination with understanding the effects of UVB light exposure dates back nearly a century, there is little known about the effects of exposure to longer wavelengths of light (visible light). An interesting question regarding the effects of long wavelength light exposure in the skin arises when one considers the wavelength induction of melanoma within select interspecies hybrids of *Xiphophorus* fish. Exposure of these animals to visible light after UVB exposure is able to reduce melanoma induction to

background levels. This is thought to be largely due to the removal of UVB induced photoproducts within their DNA by photoenzymatic repair, a light driven DNA repair process. Whether visible light exposure on its own induces a unique molecular response within *Xiphophorus* species is still an unanswered question. To identify the transcriptional responses that occur within the skin of *X. maculatus* Jp 163 B after UVB and/or photoreactivating light (PRL) exposure, next generation RNA sequencing (RNAseq) was employed (Chapter 3).

In chapter 3 we presented RNAseq results that identified genes that possessed significantly altered expression values in the skin of *X. maculatus* Jp 163 B after UVB, UVB and PRL, or only PRL exposure. Here we present the placement of a subset of these genes (those with $\log_2FC > 2$ and P val < 0.01) into biological pathways using gene clustering and functional ontology tools. The first tool used for comprehensive functional analysis was David Bioinformatics (<http://david.abcc.ncifcrf.gov>, Huang *et al.*, 2009). This online resource provides gene-annotation enrichment analysis in addition to functional annotation clustering of large gene sets. Although some of the genes analyzed were grouped into multiple biological pathways, those with the most significant P value enrichment scores were selected. This was done to place each gene into only the strongest correlated biological pathway. In addition to DAVID Bioinformatics, STRING (<http://string-db.org>) was used to visualize interactions among genes. STRING is a program that predicts both direct (physical) and indirect (functional) gene product interactions. The nodes that connect each of the proteins within each STRING image have a thickness and length that is based on a gene interaction enrichment score. Therefore, both thicker and shorter connecting nodes indicate a stronger association.

Results:**A) Identification of biological pathways modulated by UVB exposure in the skin of *X. maculatus* Jp 163 B.**

In order to identify biological pathways within *X. maculatus* Jp 163 B skin that are modulated by UVB exposure (6.4 kJ/m² UVB) both gene clustering and functional ontology tools were used. The genes chosen for analysis were those that by DESeq analysis had a log₂FC>2 and P < 0.01 comparing normalized read counts present within UVB exposed skin vs. SHAM exposed skin. This gene set has a total of 131 up- and 34 down-regulated genes.

Analysis of 131 UVB up-regulated genes by DAVID Bioinformatics resulted in the clustering of 70 genes into 8 unique biological groups (Tables 4-1 and 4-2). There were two biological groups that shared the highest enrichment score (P value of 1.8E⁻⁰³); these were “stress response” and “EGFR signaling”. The group with the highest number of genes (23 total) was denoted as “transcription regulatory activity”. Of the 131 UVB up-regulated genes, 72 were found to have significant interactions by STRING analysis (Figure 4-1).

Analysis of the 34 UVB down-regulated genes by DAVID Bioinformatics resulted in the clustering of 31 genes into 4 biological groups (Tables 4-3 and 4-4). The group with the highest enrichment score (2.7E⁻⁰⁶) and greatest number of genes (13 total) were involved with the “cell cycle”. Out of the same 34 UVB down-regulated genes, 21 were found to have significant interactions by STRING analysis (Figure 4-2).

Table 4-1: DAVID functional analysis clustering of up-regulated genes in UVB exposed (6.4 kJ/m^2 UVB) skin of *X. maculatus* Jp 163 B. A total of 131 genes that had a $\log_2\text{FC} > 2$ and $P < 0.01$ were used for this analysis and 73 were grouped into the biological groups listed in the table. Each gene is represented by a single annotation cluster based on an annotation cluster enrichment score (P value).

Annotation Cluster ID	Number of Genes	P value
Stress response	4	$1.80 \cdot E^{-03}$
EGFR signaling	6	$1.80 \cdot E^{-03}$
Regulation of actin cytoskeleton	11	$4.40 \cdot E^{-03}$
Peptidase activity	12	$4.60 \cdot E^{-03}$
Melanosome	4	$5.30 \cdot E^{-03}$
Carbohydrate binding	6	$6.30 \cdot E^{-03}$
Transcription regulator activity	23	$7.00 \cdot E^{-03}$
Cell surface receptor signal transduction	6	$9.50 \cdot E^{-03}$

Table 4-2: List of genes placed within multiple biological categories after DAVID functional analysis clustering of up-regulated genes in UVB exposed (6.4 kJ/m² UVB) skin of *X. maculatus* Jp 163 B.

Stress response

CIRBP, HSPB1, HSPB7, HSPB6

EGFR signaling

CBL, CDKN1B, GSK3B, PIK3R1, SOS1, CRKL

Regulation of cytoskeleton

BAIAP2L2, ADD3, CFL2, FSCN1, HIP1, MYPN, MYBPC2, MYBPC2, MYLK, MYL2, MYL4, TCAP

Peptidase activity

ENDOU, CPA1, CPA3, CPA4, CTRC, CELA1, CTRB2, LTA4H, PRSS23, PRSS3, RHBDL2, USP13

Melanosome

CTSD, FLOT1, HSP90AA1, YWHAE

Carbohydrate binding

DGCR2, APP, CEL, GYG1, LPL, SPOCK3

Transcription regulator activity

APEX1, ELK3, KLF9, RAD54L2, RBM14, JUNB, TSC22D1, YAPI, ATF4, ATF5, FUBP3, FOXK2, HMGB2, MKL1, NFIX, SUPT5H, TFAP4, MAFB, ZNF207, ZNF281, ZFP36L1, JUN

Cell surface receptor signal transduction

APC, CXCL12, F2RL2, FSTL1, GHR, ITGB5, SLC26A6, ZFP106

Table 4-3: DAVID functional analysis clustering of down-regulated genes in UVB exposed (6.4 kJ/m^2 UVB) skin of *X. maculatus* Jp 163 B. A total of 34 genes that had a $\log_2\text{FC} > 2$ and $P < 0.01$ were used for this analysis and 31 were placed into the biological groups as listed in the table. Each gene is represented by a single annotation cluster based on an annotation cluster enrichment score (P value).

Annotation Cluster	Number of Genes	P value
Cell cycle	13	$2.70 \cdot E^{-06}$
DNA replication	7	$4.20 \cdot E^{-03}$
Actin binding	5	$8.60 \cdot E^{-03}$
Intracellular signaling cascade	6	$8.70 \cdot E^{-03}$

Table 4-4: List of genes placed within multiple biological categories after DAVID functional analysis clustering of down-regulated in UVB exposed (6.4 kJ/m² UVB) skin of *X. maculatus* Jp 163 B.

Cell cycle

PBK, SPC24, ANXA1, MKI67, BIRC5, CENPF, CCNB1, CCNB3, HSD3B7, INCENP, IL12B, PSME2, GADD45B

DNA replication

PNP, CENPF, POLD2, POLE, POLD3, TK1, POLR2H

Actin binding

CXCR4, DBNL, MYBPC2, ARPC3, KRT23

Intracellular signaling cascade

TIAM1, CXCR4, CHRM5, DBNL, MCTP2, RGL3

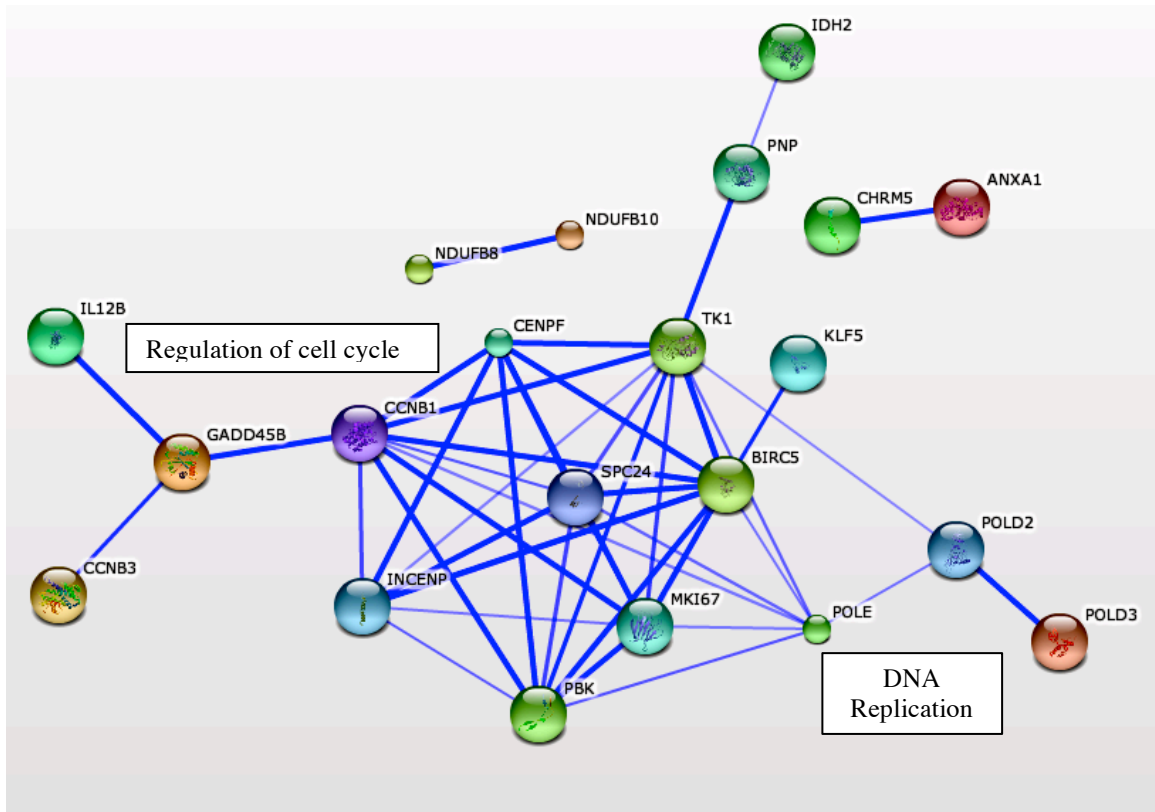


Figure 4-2: STRING analysis of significant ($P < 0.01$) down-regulated genes in UVB exposed (6.4 kJ/m^2 UVB) skin of *X. maculatus* Jp 163 B. A total of 34 genes were entered into STRING for analysis and of these, 21 were clustered based on both direct (physical) and indirect (pathway) protein interactions. The thickness of each line represents the amount of confidence between the protein interactions (enrichment score). The spatial arrangement of each protein within the image is also indicative of how closely associated they are to one another.

C) Identification of biological pathways modulated by PRL exposure in the skin of *X. maculatus* Jp 163 B.

In order to identify biological pathways within *X. maculatus* 163 B skin that are modulated solely by photoreactivating light (PRL) exposure both gene clustering and functional ontology tools were used. Genes chosen for this analysis were those that were previously determined by DESeq analysis to have expression values of $\log_2FC > 2$ and $P < 0.01$ comparing normalized read counts present within the PRL exposed (2 hrs PRL) skin vs. SHAM exposed skin. A total of 383 up-regulated genes and 366 down-regulated genes were chosen for functional analysis by DAVID and STRING.

Analysis of the 383 PRL up-regulated genes using DAVID resulted in the clustering of 126 genes into 7 unique biological groups (Tables 4-9 and 4-10). The group that had the highest enrichment score (P value of $3.20 \cdot E^{-11}$) was “Src homology domain” and the group with the highest number of genes (26 total) involved “cell adhesion”. Analysis of the same 383 PRL up-regulated genes by STRING identified significant interactions among 125 genes (Figure 4-4).

Analysis of the 366 PRL down-regulated genes resulted in the clustering of 101 genes into 9 biological groups (Tables 4-11 and 4-12). The group that possessed the highest enrichment score (P val of $2.90 \cdot E^{-09}$) involved the “cell cycle” and the group with the highest number of genes (27 total) associated with the “cytoskeleton”. Analysis of the same 366 PRL down-regulated genes by STRING identified significant interactions among 78 genes (Figure 4-4).

Table 4-5: DAVID functional analysis clustering of up-regulated genes in PRL exposed (2 hrs PRL) skin of *X. maculatus* Jp 163 B. A total of 383 genes that had a $\log_2FC > 2$ and were used for this analysis. One hundred and twenty six genes were placed into biological groups listed in the table. Each gene is represented by a single annotation cluster based on a annotation cluster enrichment score (P value).

Annotation Cluster ID	Number of Genes	P value
Src homology domain	22	$3.20E^{-11}$
Cell adhesion	29	$8.70E^{-10}$
Immune response	25	$4.90E^{-09}$
Biological rhythm	11	$5.50E^{-07}$
Plekstrin homology	14	$2.20E^{-05}$
Extracellular matrix	16	$2.50E^{-05}$
Response to hormone stimulus	9	$1.30E^{-03}$

Table 4-6: List of genes placed within multiple biological categories after DAVID functional analysis clustering of up-regulated genes in PRL exposed (2 hrs PRL) skin of *X. maculatus* Jp 163 B.

Src homology domain

CASS4, FYN, ARHGAP4, SH3BP4, SLA, ABI1, DOCK4, DBNL, HCK, MPP3, NPHP1, NCF1, NCF2, NCF4, PLCG2, PSTPIP1, SKAP2, TEC, TNK2, UBASH3B, CRKL, LYN

Cell adhesion

ADAM15, ADAM8, ADAM9, CD2, CD22, CD44, CD6, CD97, L1CAM, RAPH1, ARHGAP6, SOX9, APBA1, CSF3R, EMB, INPPL1, ITGA4, ITGAL, ITGB2, LPXN, MAGII, MYBPC3, PLEK, PLXNC1, PVRL1, PCDH18, SIGLEC1, SDK1, SYK

Biological rhythm

ADAMTS1, DBP, ARNTL2, CRY1, CRY2, MSTN, PRF1, PER1, PER3, TEF, TGFB3

Immune response

BLNK, GPR68, AIF1, C1QA, C1QC, C2, CDO1, CYBB, HMOX1, IDO1, IL6R, CD79A, CXCR1, KDM6B, LYZ, P2RX7, RIPK2, TLR2, TLR8, UNC13D, JAK2, ENTPD2, BCL6, GPR183, CXCR5

Extracellular matrix

ANGPTL4, PMF1, COL1A1, COL1A2, COL2A1, COL5A1, COL5A2, COL6A1, COL10A1, COL22A1, FBLN2, MMP9, SPARC, SPON2, TGFBI, WNT10B

Plekstrin homology

FGD5, GAB3, RASAL2, ARHGAP15, ARHGAP22, ARHGAP25, SWAP70, APBB1IP, CERK, DGKD, DOK3, DAPPI, PLEKHF1, PLEKHM3

Response to hormone stimulus

ABCA2, ABCC5, ADH1A2, DOM3Z, FOXO1, GNB3, OSMR, PTGS1, PTPN1

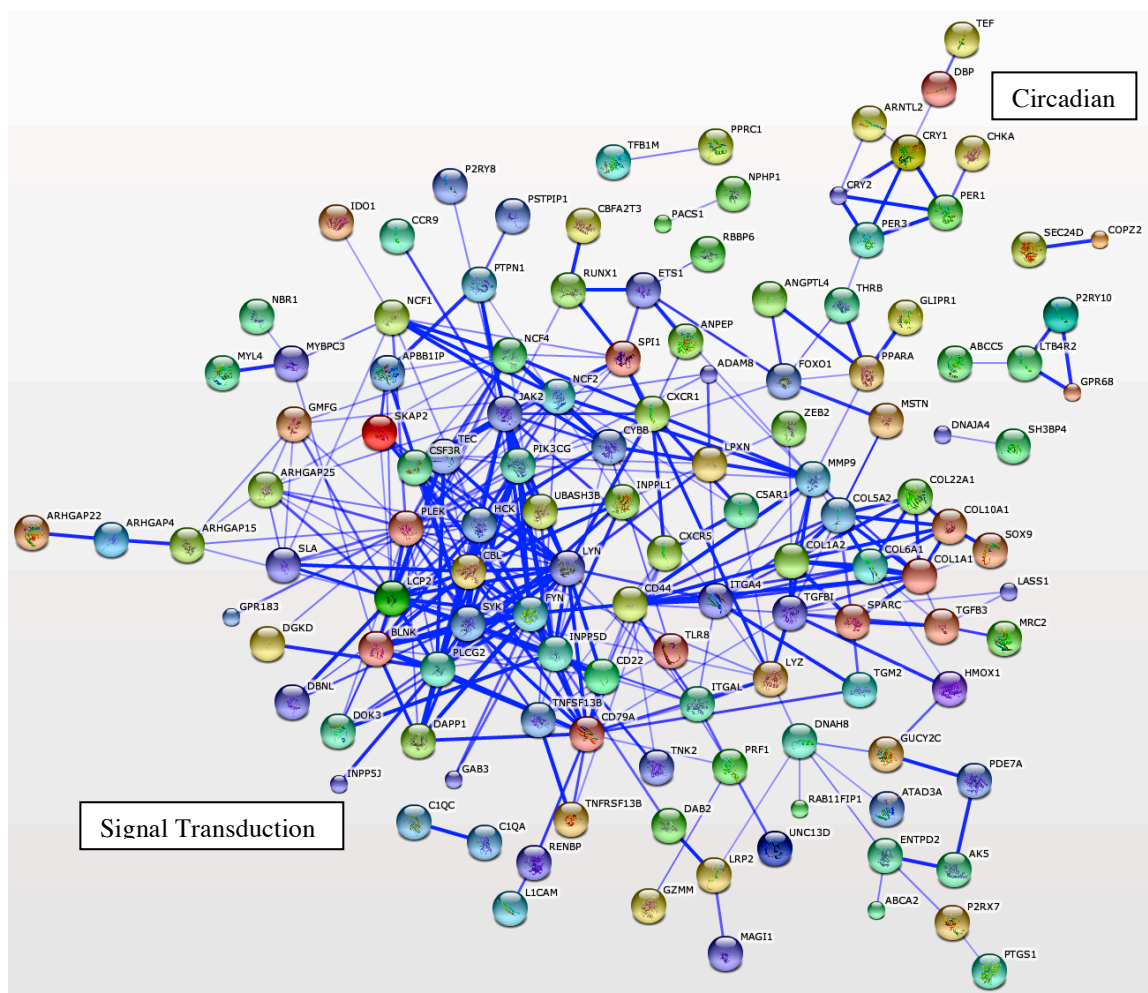


Figure 4-3: STRING analysis of significant ($P < 0.01$) up-regulated genes in PRL exposed (2 hrs PRL) skin of *X. maculatus* Jp 163 B. A total of 383 genes were entered into STRING for analysis and of these 125 were clustered based on both direct (physical) and indirect (pathway) protein interactions. The thickness of each line represents the amount of confidence between the protein interactions (enrichment score). The spatial arrangement of each protein within the image is also indicative of how closely associated they are to one another.

Table 4-7: DAVID functional analysis clustering of down-regulated genes in PRL exposed (2 hrs PRL) skin of *X. maculatus* Jp 163 B. A total of 396 genes that had a $\log_2FC > 2$ were used for this analysis and 96 were placed into 9 biological groups. Each gene is represented by a single annotation cluster based on an annotation cluster enrichment score (P val < .001).

Annotation Cluster	Number of Genes	P value
Cell cycle	26	2.90E ⁻⁰⁹
Cytoskeleton	27	3.80E ⁻⁰⁶
GTPase binding	9	5.80E ⁻⁰⁵
Epidermis development	11	7.80E ⁻⁰⁴
Fos transforming protein	4	6.30E ⁻⁰³
Chromoprotein	4	4.90E ⁻⁰³
Transcription regulator activity	11	6.50E ⁻⁰³
Axon guidance	4	8.50E ⁻⁰³
Oxidoreductase	4	9.00E ⁻⁰³

Table 4-8: List of genes placed within multiple biological categories after DAVID functional analysis clustering of down-regulated genes in PRL exposed (2 hrs PRL) skin of *X. maculatus* Jp 163 B.

Cytoskeleton
<i>PDLIM5, ABLIM1, CBX1, CORO1C, ENC1, EPB41L4B, ESPL1, FILIP1L, KRT23, KIF20A, KY, MYO5C, MYBPC2, NTRK2, PNP, PLEK2, RAPSN, SYNC, STX1A, TEKT1, TNNI1, TNNI2, TNNT2, USP2, MYC, ZYX</i>
Cell cycle
<i>HAUS2, MAD2L1, MTBP, NEK2, SPC24 MKI67, BIRC5, CASC5, CDK1, CDC20, CETN3, CEP55, CCDC99, CCNB1, CCNF, CCNG2, KIFC1, KNTC1, MCM8, NCAPG2, NUSAP1, PRC1, RGS2, SASS6, TP73</i>
GTPase binding
<i>NOXA1, DIAPH3, ECT2, EPOR, FMNL1, RPH3A, RGL3, RIMS2, SYTL2</i>
Epidermis development
<i>ELF3, KLF4, ANXA1, COL5A3, EDAR, FOXN1, FOXQ1, HOXC13, FGF7, PTGS2, TXNIP</i>
Fos transforming protein (1.0E-3)
<i>FOSB, FOS, JDP2</i>
Chromoprotein
<i>CYP1A1, CYP1A2, CYP1B1, CYB5A</i>
Transcription regulator activity
<i>ARID5A, ELF3, KLF2, TBX18, AR, AHRR, DLX3, EHF, FHL5, HOXA11</i>
Axon guidance
<i>GFRA3, DAB2, ALCAM, NRXN1</i>
Oxidoreductase
<i>BCO2, HSD3B7, IDH2, PRODH</i>

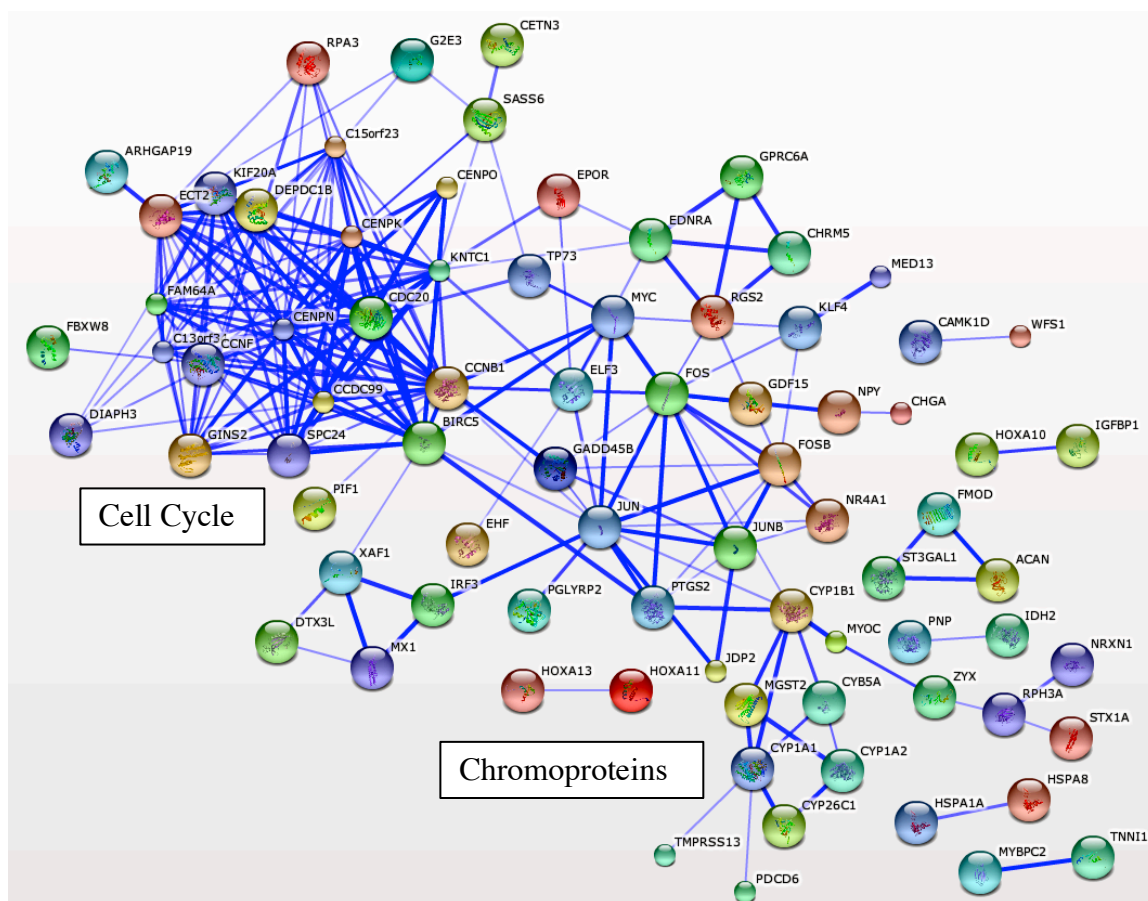


Figure 4-4: STRING analysis of significant ($P < 0.01$) down-regulated genes in PRL exposed (2 hrs PRL) skin of *X. maculatus* Jp 163 B. Three hundred sixty-six genes were entered into STRING for analysis and out of these, 78 were clustered based on both direct (physical) and indirect (pathway) protein interactions. The thickness of each line represents the amount of confidence between the protein interactions (enrichment score). The spatial arrangement of each protein within the image is also indicative of how closely associated they are to one another.

D) Identification of biological pathways modulated by UVB + PRL exposure in the skin of *X. maculatus* Jp 163 B.

In order to identify biological pathways within *X. maculatus* 163 B skin that are modulated by UVB + PRL exposure, DAVID and STRING gene clustering and functional ontology tools were used. Fish within this group were exposed to the same UVB dose (6.4 kJ/m²) as above (section B, UVB) but in addition also received exposure to 2 hrs of PRL. The genes chosen for analysis were those that were previously determined by DESeq analysis to have $\log_2FC > 2$ and $P < 0.01$ by comparing normalized read counts present within UVB + PRL exposed skin vs. SHAM exposed skin. A total of 98 up- and 229 down-regulated genes were chosen for functional analysis by DAVID and STRING.

Functional analysis of the 98 up-regulated genes by DAVID Bioinformatics resulted in the clustering of genes into 7 biological groups (Tables 4-4 and 4-5). The group with the highest enrichment score (p value of $1.4 \cdot E^{-06}$) was the “nucleolus” while the group with the highest number of genes (29 total) is involved in “transcriptional regulation”. Of the 98 up-regulated genes, 62 were found to have significant interactions by STRING analysis (Figure 4-3).

Functional analysis of the 229 down-regulated genes by DAVID resulted in the clustering of 88 genes into 7 biological groups (Tables 4-4 and 4-5). The group with the highest enrichment score (p value of $2.1 \cdot E^{-08}$) is the “extracellular matrix” and the group with the highest number of genes (18 total) is involved with the “cell cycle”. Of the same 229 down-regulated genes, 60 were found to have significant interactions by STRING analysis (Figure 4-4).

Table 4-9: DAVID functional analysis clustering up-regulated genes in UVB + PRL (6.4 kJ/m² UVB + 2 hrs PRL) exposed skin of *X. maculatus* Jp 163 B. A total of 98 genes had a log₂FC > 2 and P < 0.01 and were used for this analysis. Eighty-eight genes were placed into the biological groups listed above. Each gene is represented by a single annotation cluster based on an annotation cluster enrichment score (P value).

Annotation Cluster ID	Number of Genes	P value
Nucleolus	17	1.40·E ⁻⁰⁶
Ribosome biogenesis	11	1.10·E ⁻⁰⁵
Biological rhythm	6	9.80·E ⁻⁰⁵
Endoplasmic reticulum membrane	13	2.30·E ⁻⁰⁴
Polyamine metabolic process	4	4.50·E ⁻⁰⁴
Transcription regulation	29	1.30·E ⁻⁰³
Receptor protein tyrosine kinase signaling	8	5.40·E ⁻⁰⁴

Table 4-10: List of genes placed within multiple biological categories after DAVID functional analysis clustering of up-regulated genes in UVB + PRL exposed (6.4 kJ/m² UVB + 2 hrs PRL) skin of *X. maculatus* Jp 163 B.

Nucleolus (1.40E-06)

DDX47, DDX54, ELK3, GLIS1, NMD3, RBM14, SOX9, CIRH1A, CCNT2, IPO5, NAV2, NOC2L, NOC4L, PDK2, TXN2, ZFP106, ZNF207

Ribosome biogenesis (1.10E-05)

BMS1, HEATR1, IMP4, NOP2, BYSL, DKC1, FBL, NAF1, NOLC, PDCD11, RPS14

Biological rhythm (9.80E-05)

ARNTL2, CRY1, CRY2, PER1, PER2, PER3

Endoplasmic reticulum membrane (2.30E-04)

DHCR7, ARL6IP1, ATP2A2, NOMO1, SEC24C, SEC24D, SEC61A1, WFS1, RPN1, SSR2, ACER2, SGPL1, SREBF1

Polyamine metabolic process (4.50E-04)

AMD1, AZIN1, ODC1, SMOX

Transcription regulation (1.30E-03)

CEBPZ, DENND4A, HBPI, KHSRP, KLF11, PHF20, RUVBL2, SRCAP, TSC22D1, XBPI, ATF4, BAZ1A, FUBP3, FSTL3, FOXK2, HDAC9, HIVEP2, IRX3, JARID2, NFIX, PPRC1, PRMT5, SUPT5H, SUZ12, TFAP4, MAFB, ZNF281, ZNF800, ZXDA

Receptor protein tyrosine kinase signaling (5.40E-03)

FOXO4, GRB10, GHR, NRP1, PTPN1, SIK2, SOS1, SOCS5

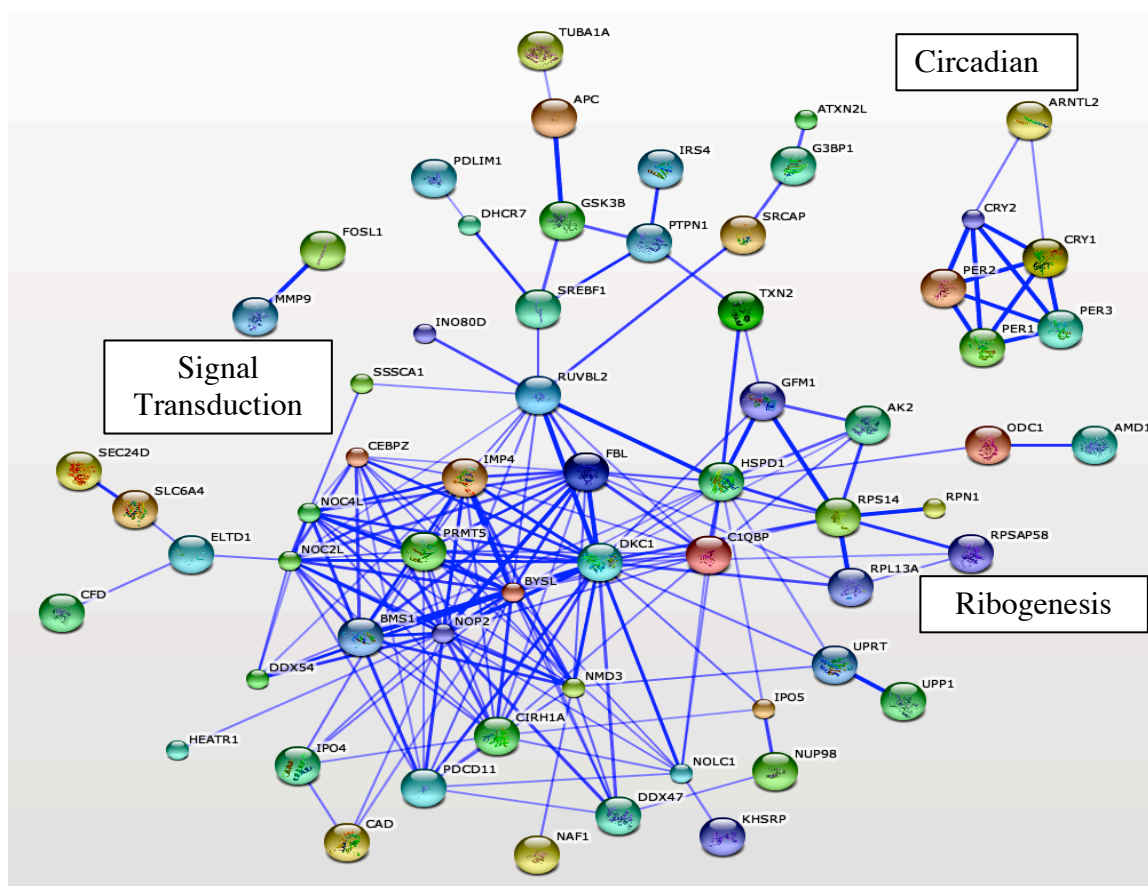


Figure 4-5: STRING analysis of significant ($P < 0.01$) up-regulated genes in UVB + PRL (6.4 kJ/m^2 UVB + 2 hrs PRL) exposed skin of *X. maculatus* Jp 163 B. Ninety-eight genes were entered into STRING for analysis and of these 62 were clustered based on both direct (physical) and indirect (pathway) protein interactions. The thickness of each line represents the amount of confidence between the protein interactions (enrichment score). The spatial arrangement of each protein within the image is also indicative of how closely associated they are to one another.

Table 4-11: DAVID functional analysis clustering of down-regulated genes in UVB + PRL (6.4 kJ/m² UVB + 2 hrs PRL) exposed skin of *X. maculatus* Jp 163 B. A total of 229 genes that had a log₂FC > 2 and P < 0.01 were used for this analysis. Eighty-six were grouped into the biological groups listed in the table. Each gene is represented by a single annotation cluster based on an annotation cluster enrichment score (P value).

Annotation Cluster ID	Number of Genes	P value
Extracellular matrix	10	2·10E ⁻⁰⁸
Secreted	12	2·40E ⁻⁰⁸
Cell cycle	18	4·70E ⁻⁰⁶
Protease	14	3·00E ⁻⁰⁴
Mesenchymal cell differentiation	5	1·00E ⁻⁰³
Epidermis development	7	1·10E ⁻⁰³
Cell motion	12	6·20E ⁻⁰³
Chromoprotein	3	5·60E ⁻⁰³
GTPase binding	5	9·80E ⁻⁰³

Table 4-12: List of genes placed within multiple biological categories after DAVID functional analysis clustering of down-regulated genes in UVB + PRL exposed (6.4 kJ/m² UVB + 2 hrs PRL) skin of *X. maculatus* Jp 163 B.

Extracellular matrix
<i>ASPN, COL9A3, COL5A2, COL5A3, COL10A1, COL11A2, COL14A1, FMOD, FBLN2, LAMB4</i>
Secreted
<i>ST3GAL1, CYTL1, FETUB, LOXL4, NOTUM, OLFML3, PRF1, PDGFC, PRG4, TCTN1, FREM2, MATN1</i>
Cell cycle
<i>EGFL6, NEK2, PBK, SETD8, SPC24, MKI67, BIRC5, CDC20, CENPF, CEP55, CCNB3, CCNF, FOXM1, INCENP, KPNA2, PRC1, SPAG5, TACC3</i>
Peptidase activity
<i>ADAM12, CPA3, CTSH, ECE1, ESPL1, GZMM, HABP2, MMP11, MMP17, MMP19, PLAU, PRSS3, TMPRSS13, USP2</i>
Mesenchymal cell differentiation
<i>BMP2, BMP7, CYP26C1, EDNRA, NRTN</i>
Epidermis development
<i>CRABP2, COL1A1, EDAR, FOXN1, FGF7, PTCH2, TCF15</i>
Cell motion
<i>GFRA3, BMPR1B, CCL25, DNAH11, EFNA2, ALCAM, NPY, PLA2G10, TNN, VASP, KIF22, KIFC1</i>
Chromoprotein
<i>CYP1A1, CYP1A2, CYP1B1</i>
GTPase activity
<i>RILP, DIAPH3, FMNL1, RGL3</i>

D.) Verification of RNA-seq expression analysis by quantitative real-time PCR.

In order to verify a subset of RNA-seq gene expression values calculated by DESeq, quantitative real-time PCR was employed (Figure 4-7). The genes chosen for analysis were four members of the *AP-1* family of transcription factors (*JUN*, *JUNB*, *FOS*, *FOSB*) and a photolyase gene (CPD photolyase gene). In UVB exposed skin, the expression of both versions of *JUNA* and *JUNB* was up-regulated (> 3 fold), while expression of *FOS* and *FOSB* was down-regulated (< 2 fold), relative to unexposed SHAMs kin. Exposure to UVB + PRL and only PRL, resulted in the down-regulated expression of the *JUNA* and *JUNB* genes in addition to *FOS* and *FOSB*. PRL exposed skin however, possessed the greatest down-regulation in all *AP-1* genes, relative to UVB + PRL. Expression of the CPD photolyase was the highest in UVB + PRL exposed skin (7.2 fold), but was also up-regulated in skin exposed to only PRL (3.8 fold). UVB exposed skin did not display significant up-regulation of the CPD-photolyase gene compared to UVB + PRL and PRL exposed skin.

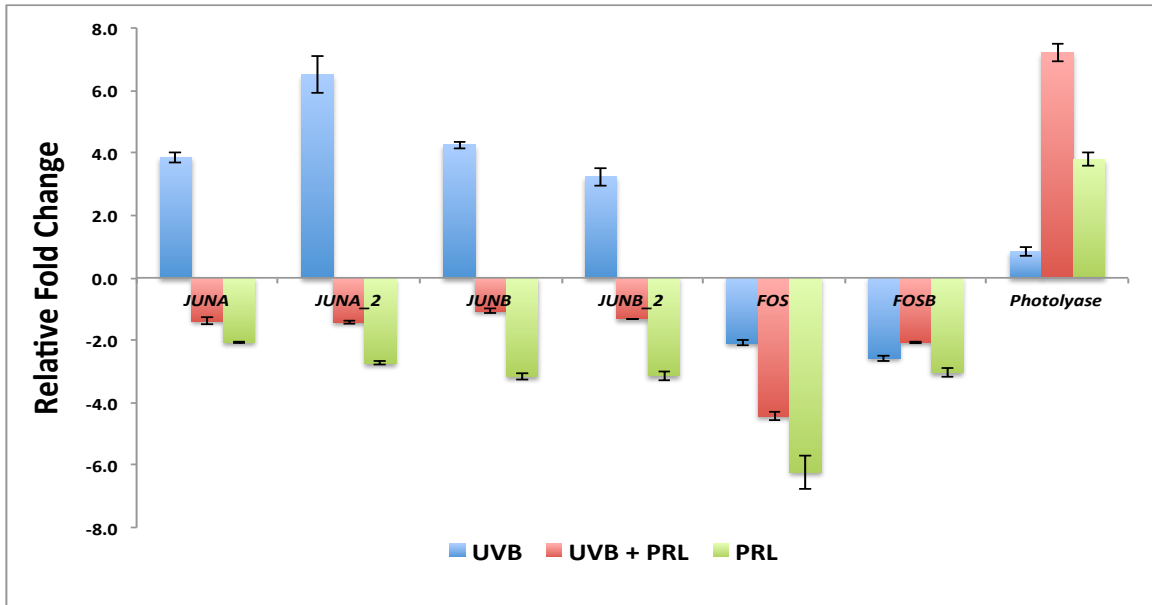


Figure 4-7: Quantitative real-time PCR analysis of verification of RNA-Seq data. Gene expression values were determined in UVB (6.4 kJ/m²), UVB + PRL (6.4 kJ/m² UVB + 2 hrs PRL), and PRL (2 hrs PRL) exposed skin of *X. maculatus* Jp 163 B. Two versions of *JUN* (*JUN* and *JUN_2*) and *JUNB* (*JUNB* and *JUNB_2*) exist in *X. maculatus* Jp 163 B, to ensure amplification of only one gene, primers were designed in non-homologous regions determined by nucleotide sequence alignments. Standard error values were determined by technical triplicate.

Discussion:

The emergence of next generation RNA-Seq technology within recent years has provided scientists with the opportunity to dissect biological processes by quantifying global changes in gene expression. Herein, we present use of RNA-Seq to study gene expression profiles in the skin of *X. maculatus* Jp 163 B after UVB, UVB + PRL, and PRL exposure. Previously (chapter 3) genes that exhibited significant changes in gene expression within the skin of *X. maculatus* Jp 163 B after UVB, UVB + PRL, or only PRL exposure were identified by DESeq analysis. In this chapter, a subset of genes within each exposed skin sample (those with a $\log_2FC > 2$ and $P < 0.01$) were placed into biological groups using two different functional annotation tools; DAVID Bioinformatics and STRING. DAVID Bioinformatics provides gene-annotation enrichment analysis and functional annotation clustering of the gene sets, while STRING assembles a visual display of direct (physical) and indirect (functional) protein interactions. These results highlight wavelength specific modulation of multiple biological pathways in the skin of *X. maculatus* Jp 163 B after UVB and/or PRL exposure.

The UVB portion of solar ultraviolet light accounts for the majority of the harmful effects induced by prolonged sunlight exposure. UVB exposure can cause direct DNA damage in the form of UV photoproducts (CPDs and [6-4]PDs) as well as activate critical molecular targets and signal transduction pathways that in turn result in altered gene expression. Exposure of adult male *X. maculatus* Jp 163 B to narrow band UVB (~311 nm) resulted in both DNA damage (CPDs and [6-4]PDs) as we determined by RIA analysis (chapter 2), and induced significant changes in gene expression. A total of 912 genes (chapter 3) were determined to show significantly modulated expression values

after UVB exposure. Of these genes, 449 were up- and 493 were down-regulated. From the set 131 up- and 34 down-regulated genes were chosen for functional annotation analysis based on exhibiting a fold change cutoff of $\log_2FC > 2$ at $P < 0.01$ (i.e., about a 4 fold change in expression).

Functional analysis of the 131 up-regulated genes using DAVID resulted in the placement of 73 genes into 8 biological group (4-1). The biological groups included stress response, EGFR signaling, regulation of cytoskeleton, peptidase activity, melanosome, carbohydrate binding, transcription regulatory activity, and cell surface receptor signal transduction. Two groups (i.e., stress response and EGFR signaling) shared the highest enrichment score. Genes within the stress response group respond to disturbances in cellular homeostasis, such as changes in temperature, oxygen tension, radiation exposure, or wounding. Three genes within this group (*HSPB1*, *HSPB7* and *HSPB6*) are molecular chaperones within the heat shock family of proteins. UVB is known for its ability to damage cellular components, such as DNA and proteins, and this may provide an explanation for the up-regulation of these protective chaperone genes. Also, genes within the “peptidase activity” group were induced that may provide for degradation of UVB or ROS damaged proteins.

The second biological group within UVB up-regulated genes with the highest enrichment score was “EGFR signaling”. Genes within this group respond to a series of molecular signals that are initiated by binding of a ligand to a member of the EGFR family of receptor tyrosine kinases on the surface of the cell and initiate regulation of a downstream cellular process such as transcription or cell division. A well-known cell cycle mediator *CDKN1B*, was present within this group, in addition to two members of

the RAS signal transduction pathway (*SOS1* and *CRKL*). Members of the RAS signaling pathway participate in the regulation of cell growth and differentiation by taking part in the blockage of cell cycle progression via increasing levels of *CDKN1B* or other proteins that prevent DNA replication prior to DNA repair. Additional genes involved in signaling pathways were also identified within the “cell surface receptor and signal transduction” biological group.

The biological group within the UVB up-regulated gene set that had the largest number of genes within it is “regulation of transcription”. Genes within this biological group are able to either promote or inhibit selective gene transcription. Analysis of the transcription regulatory genes using DAVID identified *ELK3*, *SMYD1*, *SUPT5H*, *ATF5*, *APEX1*, and *ZNF281* as being general repressors of transcription and *RBMI4*, *YAP1*, *ATF4*, *JUN*, *MKLI*, *MAFB*, and *SUBT5H* as transcriptional activators. Overexpression of both activators and repressors of transcription provides an avenue for the simultaneous rapid affect of multiple biological pathways. Multiple motor proteins, including members of the myosin family of proteins (*MYPN*, *MYBPC2*, *MYLK*, *MYL2*, *MYL4*), were present within the biological group designated as “regulation of cytoskeleton”. Proteins within this biological group are involved in the transport of vesicles along microfilaments in addition to muscle cell contraction. These proteins may be involved in the transfer of various cellular components that function in extracellular matrix remodeling, a process shown to occur in the skin after UVB exposure.

Analysis of the same 131 UVB up-regulated genes by STRING resulted in the clustering of 72 genes (Figure 4-1). Although STRING does not separate gene lists into discrete biological clusters like DAVID, there were several groups of genes within

STRING produced images that shared higher enrichment values based on the thickness and length of the connecting nodes. A large cluster is present near the top of the STRING image (Figure 4-1) that consists of genes found within the DAVID biological groups “EGFR signaling” and “transcription regulatory activity”. *PIK3RI*, a lipid kinase involved in multiple signal transduction pathways was at the center of this group and had direct connections with *APP*, *F2RL2*, *KIRREL*, *PIP4K2C*, *GHR*, *CBL*, *SOS1*, *CRKL*, *IR54* and *GSK3B*. Below this group is another set of genes that are part of the “transcription regulatory activity” group. Three members of the AP-1 family of transcription factors, *JUN*, *JUNB* and *ATF4*, were present in this group and have previously been shown as central players in the UVB response of skin. Genes within the “regulation of cytoskeleton” group were grouped together to the left of the image and a new group of ribosomal proteins (*RPSAP58*, *RPS10*, *RPL13A*, *RPS14*, and *EEF2*) are clustered on the right of the STRING image. These ribosomal proteins are largely precursor proteins that after processing form mature ribosomal subunits involved in translation. With such large increases in transcription occurring, one could predict a need for additional components necessary for translation. Four genes were also present within the group “melanosome” which are associated with the genes that regulate the production of melanin and other pigments within melanocytes. *X. maculatus* Jp 163 B possesses the enhanced “spotted side” (Sp) macromelanophore pigmentation phenotype and genes within this class could function in the UV response within these pigment cells as a protective mechanism.

DAVID functional analysis of the 34 down-regulated genes within the UVB exposed sample resulted in the clustering of 31 genes into 4 biological groups. These

groups included “cell cycle”, “DNA replication”, “actin binding”, and “intracellular signaling cascade”. The group with both the highest enrichment score and highest number of genes was the “cell cycle” group. Several genes within this group are central to progression of the cell cycle at the G2/M checkpoint, including two members of the cyclin B family (*CCNB1* and *CCNB3*), *BIRC5* (also known as “survivin”), and *PBK*. Within the “DNA replication” group were three polymerase accessory subunits (*POLD2*, *POLD3*, *POLR2H*) and DNA polymerase epsilon (*POLE*). The regulation of cell cycle progression genes and DNA replication machinery would be critical upon UVB induced DNA damage, allowing time for the removal of lesions prior to DNA replication and cell division. Genes present within the “cell cycle” and “DNA replication” were also grouped together in a large STRING central cluster. There are two additional DAVID biological groups, “actin binding” and “intracellular signaling cascade”, however these genes were not clustered as interacting together by STRING.

Although many studies have investigated the antitumorigenic effect of PER within UV-inducible melanoma models, including *Xiphophorus*, there is little knowledge about the transcriptional responses that occur during this process in the skin. To address this, a subset of UVB exposed *X. maculatus* Jp 163 B were also exposed to two hours of photoreactivating light (PRL) to study gene expression changes under PER conditions. Within UVB + PRL exposed skin, a total of 2,099 genes were determined to have significant expression fold change values, of which 866 were up-regulated and 1,231 were down-regulated (chapter 3). Of these, 98 up-regulated and 229 down-regulated genes were chosen for functional annotation analysis based on a fold change cutoff of $\log_2FC > 2$ ($P < 0.01$). Functional analysis by DAVID resulted in the placement of 88 of

the up-regulated genes into 7 biological groups (Table 4-5). These groups included nucleolus, ribosome biogenesis, biological rhythm, endoplasmic reticulum membrane, polyamine metabolic process, transcription regulation, and receptor protein tyrosine kinase signaling.

The biological group with the highest enrichment score was the “nucleolus” group containing genes involved in the formation of ribonucleoprotein precursors that mature into the 40S and 60S subunits of the ribosome. A similar biological group, “ribosome biogenesis”, was also identified that contained genes similarly involved in the synthesis of ribosomal precursors and the regulation of translation. A ribosomal group was also present within the UVB exposed skin sample, although the genes within this group did not match those of the UVB + PRL groups discussed above. The biological group with the highest number of proteins was “transcriptional regulation” containing several genes also up-regulated within the UVB exposed sample. Common transcription regulators between the two data sets (UVB and UVB + PRL) included *TSC22D1*, *ATF4*, *FUBP3*, *FOXK2*, *NFIX*, *SUPT5H*, *TFAP4*, *MAFB*, and *ZNF281*. The up-regulation of these genes under both exposure conditions (UVB and UVB + PRL) in the skin of *X. maculatus* Jp 163 B may indicate their participation in a general response to UVB, even after post exposure to longer wavelengths of light (PRL) and the resulting photoproduct removal.

Several circadian genes were also up-regulated by UVB + PRL exposure and placed within the “biological rhythm” group. Four of these genes (*PER1*, *PER2*, *PER3*, and *ARNTL2*) are involved in the mammalian circadian cycle and two are photolyase-like genes (*CRY1* and *CRY2*). All of these genes were also grouped in a cluster by STRING analysis. As indicated by the previously published RIA results, *X. maculatus* Jp 163 B is

capable of photoenzymatic repair (PER) of both CPDs and (6-4)PDs, however whether these two photolyase genes (designated *CRY1* and *CRY2*) are indeed the photolyases responsible for PER in the skin requires further experiments. It is possible that *Xiphophorus* fish possess both functional and non-functional (photoperiodism) photolyase-like genes that were not identified within this data set.

Functional analysis of the 229 genes down-regulated after UVB + PRL exposure by DAVID resulted in the placement of 83 genes into 9 biological groups (table 4-7). The group with the highest enrichment score was the “extracellular matrix” and it contained multiple collagen proteins (*COL5A2*, *COL10A1*, and *COL11A2*) as well as a collagen assembly gene (*FMOD*). There were additional genes involved in extracellular remodeling present within the “peptidase activity” group, including *HABP2*, *MMP11*, *MMP17*, and *MMP19*. Two biological groups related to skin physiology were also present; these were “epidermis development” and “mesenchymal cell differentiation”. Genes within the epidermal development group promote the production of specific extracellular material that make up the outermost layer of the skin and mesenchymal cells are a component of the connective tissue found within the skin. Three members of the cytochrome p450 type 1 family of proteins (*CYP1A1*, *CYP1A2*, and *CYP1B1*) were placed in the “chromoprotein” cluster by DAVID and also clustered by STRING. These proteins are largely involved in the metabolism of aryl hydrocarbons, including hormones, and are thought to be light sensitive (Luecke *et al.*, 2010). Genes present within the “cell cycle” group were common to those down-regulated in the UVB exposed skin sample. These shared down-regulated cell cycle genes included *MKI67*, *CENPF*, *INCENP*, *CCNB1*, *BIRC5*, *SPC24*, and *PBK*. Although fish within this group were

exposed to PRL after UVB, promoting PER of UV photoproducts, the down-regulation of these cell cycle progression genes may be part of a general UVB response.

Exposure of *X. maculatus* 163 B to only PRL (2 hrs visible light) resulted in the greatest number of molecular genetic changes in the skin. This may not be surprising when one considers the daily changes in lighting conditions that represent important adaptive cues used for orientation in the environment and the coordination of physiological responses needed by fishes. A total of 4,027 gene transcripts were determined to have significant gene expression fold change values after normalized RNA read counts in the PRL sample were compared to those in SHAM exposed samples. Of these 4,027 genes, 2,776 were up-regulated and 1,551 were down-regulated. For functional analysis, 383 of the up-regulated genes and 366 of the down-regulated genes were chosen based on a fold change cutoff of $\log_2FC > 2$ ($P < 0.01$).

Analysis of the PRL 383 up-regulated genes by DAVID resulted in the placement of 89 genes into 8 biological groups (Table 4-9). These groups included “src homology domain”, “cell adhesion”, “biological rhythm”, “immune response”, “extracellular matrix”, “plekstrin homology”, and response to “hormone stimulus”. The group with the highest enrichment score was “src homology domain”. Genes within this group contain a protein domain of about 50 amino acids that is a conserved sequence found within the non-catalytic part of enzymes such as phospholipases and tyrosine kinases, such as SRC. SRC homology domains are normally found in signaling proteins or adapter proteins that regulate the cytoskeleton and aid in the signal transduction of receptor tyrosine kinase pathways. Genes within the “plekstrin homology domain” also contain conserved regions found on proteins involved in intracellular signaling and regulation of the

cytoskeleton. A large cluster of genes within both the src and plekstrin homology groups was present in the STRING results, highlighting their similar roles in intracellular signal transduction after PRL exposure.

The biological group with the highest number of genes was “cell adhesion”, containing genes that aid in the attachment of cells to each other or to other substrates such as the extracellular matrix. Several members of the ADAM family of metalloproteinases (*ADAM15*, *ADAM8*, and *ADAM9*) were present within this group and are known for their involvement in extracellular remodeling and regulation of cell adhesion within the skin. Additional genes within the “extracellular matrix” group, particularly multiple collagen genes and TGFBI, also regulate cellular adhesion and remodeling of the extracellular matrix of the skin. Genes from both the cell adhesion and extracellular matrix groups were grouped together by STRING, particularly the collagen genes.

Consistent with the UVB + PRL exposed skin data, a number of biological rhythm genes were also up-regulated and grouped together both by DAVID and STRING. This group (biological rhythm) included three period genes (*PER1*, *PER2*, and *PER3*), the aryl hydrocarbon nucleation factor (*ARNTL2*), two photolyase-like genes (*CRY1* and *CRY2*), and several genes (*DBP*, *MSTN*, *TGFB3*, and *TEF*) that were not noted as differentially regulated within the UVB + PRL exposed skin involved in cellular differentiation, particularly *TGFB3*. The presence of the two photolyase-like genes within this data set is of particular interest because increases in photolyase activity in the skin after visible light exposure only has rarely been demonstrated. The up-regulation of one of these genes (*CRY2*, the CPD-photolyase) after UVB + PRL and PRL exposure was

also confirmed by quantitative real-time PCR in this study (chapter 3). Whether photolyase genes that are up-regulated by visible light in the absence of DNA damage participate in additional biological processes outside of photorepair requires further investigation.

There are 80 genes that were down-regulated after PRL exposure in the skin of *X. maculatus* Jp 163 B and these were placed into 7 biological groups by DAVID (Table 4-11). These groups included “cytosekeleton”, “cell cycle”, “GTPase binding”, “epidermis development”, “Fos transforming protein”, “transcription regulator activity”, and “oxidoreductase”. The “cell cycle group” had the highest enrichment score and contains several genes that were also down-regulated in the UVB and UVB + PRL exposed skin samples. There were 5 cell cycle genes (*SPC24*, *MKI67*, *CCNB1*, *CCNB3*, *GADD45B*, *CENPF* and *BIRC5*) that were down-regulated in all three light-exposed skin samples, and 4 genes (*CDC20*, *CEP55*, *CCNF*, and *PRCI*) that were present only in the UVB + PRL and PRL skin samples. These results are similar to investigations with other animal models such as zebrafish and mice where have light dependent suppression of cell cycle genes has been demonstrated (Tamai *et al.*, 2012; Ben-Shlomo *et al.*, 2009; Hunt *et al.*, 2007). Whether suppression of additional cell cycle genes after UVB exposure by PRL influences biological processes, such as DNA repair in the skin, is still unknown.

Multiple genes within the DAVID “epidermis development”, “GTPase binding”, and “chromoprotein” biological groups are the same as those in UVB + PRL exposed skin; and were also similarly grouped together by STRING. The down-regulation of these genes within both data sets may highlight their general responsiveness to longer wavelengths of light by skin, despite prior exposure to shorter UVB wavelengths.

Several genes that are part of the AP-1 family of transcription factors (*JUN*, *JUNB*, *FOS*, and *FOSB*) were also down-regulated by PRL exposure and were grouped within the “FOS transforming protein” and “transcription regulator activity” biological groups. UVB exposure however, resulted in the up-regulation of two of these AP-1 members (*JUN* and *JUNB*), indicating wavelength specific modulation of these genes. The expression of these AP-1 genes (*FOSB*, *FOS*, *JUN*, and *JUNB*) after UVB + PRL exposure was also confirmed by quantitative real-time PCR (chapter 3). In the skin, AP-1 functions as a major regulator of gene transcription and is part of the UV response. Its activity is able to control the expression of multiple DNA repair and signal transduction mediators, in addition to remodeling of the extracellular matrix (Angel *et al.*, 2001). The antagonistic expression of such transcription factors in the skin of *X. maculatus* Jp 163 B, after UVB and PRL exposure, may be responsible for some of the suggested wavelength specific transcriptional responses observed in these data.

Summary:

Skin cancer is one of the most common forms of cancer in the United states, and the etiology of the most deadly form of this disease, melanoma, is still poorly understood. This may in part be due to the number of experiments that have been performed with tumor cells and highly manipulated transgenic animal models that make it very difficult to examine UV induced molecular responses in normal skin prior to hyperplasia or tumorigenic progression. In this study, RNA-seq was utilized to examine molecular responses that occur within the skin of *X. maculatus* Jp 163 B after UVB exposure, UVB + photoreactivating light exposure (PRL), or only PRL exposure. Although common

fluorescent lamps (“cool white”, 4100K) were used for the PRL exposures, dramatic changes in gene expression values were observed in the skin of PRL exposed fish. Surprisingly, PRL exposure induced a much more robust response in the skin than UVB exposure.

After UVB exposure we observed genes involved in intracellular signaling, stress, pigment production, and transcriptional regulation were up-regulated, while genes involved in cell cycle progression and DNA replication were down-regulated. Skin that was exposed to UVB + PRL also contained up-regulated genes involved in intracellular signaling and the regulation of transcription, much like UVB exposed skin, however, multiple genes involved in ribosomal biogenesis and circadian control were also up-regulated. Several circadian genes were also up-regulated upon exposure to only PRL. Among these shared circadian genes, two putative photolyase genes (i.e., genes homologous to CPD photolyase and 6-4 photolyase) were identified and the induced expression of one of these genes (CPD photolyase) was verified by quantitative real-time PCR.

Numerous cell cycle genes were also down-regulated by both UVB + PRL and only PRL exposure. Reduced expression of cell cycle genes after visible light exposure has previously been observed in both zebrafish and mouse models, and is thought to be controlled by a circadian/photoperiodism feedback response (Hirayama *et al.*, 2009; Ben-Shlomo *et al.*, 2010). The light inducible changes in gene expression observed in *Xiphophorus* skin and how the various biochemical pathways affected are tied together with molecular genetic regulatory circuitry is an extremely interesting, and potentially important, area of study. In addition to identifying genes that had similar expression

responses or values after UVB and/or PRL exposure, genes that behave in an opposite manner when comparing UVB and PRL exposure were also identified. For example, two genes within the *AP-1* family of transcription factors (*JUN* and *JUNB*) were found to be significantly up-regulated after UVB exposure, but down-regulated after PRL exposure. These results were confirmed by quantitative real-time PCR analysis and highlight wavelength specific antagonistic regulation of gene expression. Further identification of genes within these data that possess similar expression profiles between the UVB and PRL exposed samples may reveal additional wavelength specific transcriptional responses in the skin of *Xiphophorus*. *Xiphophorus* offers investigators a rich, varied, and tractable genetic system of lines and species with which to further explore wavelength dependent gene expression within the intact organism where intercellular, inter-organ, tissues specific, and hormonal influences may be observed at virtually any point in the natural life cycle.

Future considerations:

Within this study, transcriptional responses within the skin of *X. maculatus* Jp 163 B after UVB, UVB + PRL and PRL exposure were characterized using Illumina RNA sequencing technology followed by bioinformatic data mining. During the course of the experiments detailed herein, a second parental species (*X. couchianus*) and an F₁ interspecies hybrid made by crossing *X. maculatus* 163 B with *X. couchianus* were also exposed to these same light sources and treatments. RNA-seq data from their skin of these fishes was also sequenced and awaits analysis. DNA damage quantification in the skin of all three of animal types revealed significant differences in the levels of induction

of both CPDs and (6-4)PDs within their skin. Significantly higher levels of both photoproducts were observed in skin of the non-pigmented species *X. couchianus*, while the heavily pigmented F₁ interspecies hybrid showed the lowest levels of UVB induced direct DNA damage.

Gene expression analysis of the RNA-seq data from *X. couchianus* may reveal further transcriptional responses that are wavelength specific (UVB or PRL responsive), DNA damage specific, or species specific. Analysis of the data from and the F₁ interspecies hybrid may reveal novel gene interactions as two parental alleles sets that have experienced 4-6 million years of divergence respond to the experimentally produced environmental stimuli. These future studies of gene interaction may allow us to better understand the UVB induction of melanoma within *X. couchianus* [*X. maculatus* Jp 163 B (x) *X. couchianus*] backcross hybrids. In past studies it has been shown that if heavily pigmented backcross hybrids are provided PRL exposure after UVB exposure, they do not develop melanomas, while those that do not receive the PRL treatment after UVB do. Although photoenzymatic repair of DNA photoproducts in the skin after PRL exposure is thought to be the major contributing factor, it is possible that PRL is also perturbs UVB induced molecular signaling events and this may also promote melanomagenesis within these animals.

LITERATURE CITED

- Beukers R., Ijlstra, J., Berends, W. (1958). The effect of U.V.-light on some components of the nucleic acids: I. Uracil, thymine. *Rec. Trav. Chim.*, 7, 423–429
- Cleaver, J. E. (1966) Photoreactivation: a radiation repair mechanism absent from mammalian cells. *Biochem Biophys Res Comm* 24, 569 –576.
- Cleaver, J. E. (1968) Defective repair replication in xeroderma pigmentosum. *Nature* 218,652– 656.
- Cleaver, J. E., Afzal, V., Feeney, L., McDowell, M., Sadinski, W., Volpe, J. P. G., Busch, D., Coleman, D. M., Ziffer, D. W., Yu, Y., Nagasawa, H., Little, J. B. 1(999) Increased UV sensitivity and chromosomal instability related to p53 function in the xeroderma pigmentosum variant. *Cancer Res* 59, 1102–1108.
- Cooper, S. J., Bowden, G. T. (2007) Ultraviolet B regulation of transcription factor families: roles of nuclear factor-kappa B (NF-kappaB) and activator protein-1 (AP-1) in UVB-induced skin carcinogenesis. *Curr Cancer Drug Targets*. 7, 325-334.
- Davenport, V., Morris, J. F., Motazed, R., Chu, A. C. (1999) p53 induction in normal human skin in vitro following exposure to solar simulated UV and UV-B irradiation. *J Photochem Photobiol B*. 49, 177-186.
- Friedberg, E.C., G.C. Walker, and W. Siede. (1995). DNA repair and mutagenesis. ASM Press, Washington, D.C.

- Friedberg, E. C. (2003) DNA damage and repair. *Nature* 421, 436-440.
- Fernandez, A. A., Paniker, L., Garcia, R., Mitchell, D. L. (2012) Recent advances in sunlight-induced carcinogenesis using the *Xiphophorus melanoma* model. *Comp Biochem Physiol C Toxicol Pharmacol.* 155, 64-70.
- Garcia, T. I, Shen, Y., Catchen, J., Amores, A., Schartl, M., Postlethwait, J., Walter. R. B. (2012) Effects of short read quality and quantity on a de novo vertebrate transcriptome assembly. *Comp Biochem Physiol C Toxicol Pharmacol* 155, 95-101.
- Gates, F. L. (1928) On nuclear derivatives and the lethal action of ultra-violet light. *Science* 68, 479-80.
- Gordon M. (1927) The genetics of a viviparous top-minnow *Platycoecilus*: The inheritance of two kinds of melanophores. *Genetics.* 12, 253–283.
- Hollaender, A., Curtis, J. T. (1935) Effect of sublethal doses of monochromatic ultraviolet radiation on bacteria in liquid suspension. *Proc Soc Exp Biol*; 33, 61–62.
- Huang da, W., Sherman, B. T., Tan, Q., Kir, J., Liu, D., Bryant, D., Guo, Y., Stephens, R., Baseler, M. W., Lane, H. C., Lempicki, R. A. (2007) DAVID Bioinformatics Resources: expanded annotation database and novel algorithms to better extract biology from large gene lists. *Nucleic Acids Res.* 35, 169-175.
- Jans, J., Schul, W., Sert, Y. G., Rijksen, Y., Rebel, H., Eker, A. P., Nakajima, S., van Steeg, H., de Gruijl, F. R., Yasui, A., Hoeijmakers, J. H., van der Horst, G. T. (2005) Powerful skin cancer protection by a CPD-photolyase transgene. *Curr Biol.* 15, 105-115.

- Jhappan, C., Noonan, F. P., Merlino, G. (2003) Ultraviolet radiation and cutaneous malignant melanoma. *Oncogene*. 22, 3099-3112.
- Kazianis, S., Gimenez-Conti, I., Setlow, R. B., Woodhead, A. D., Harshbarger, J. C., Trono, D., Ledesma, M., Nairn, R. S., Walter, R. B. (2001) MNU induction of neoplasia in a platyfish model. *Lab Invest*. 81, 1191-1198.
- Kazianis, S., Gimenez-Conti, I., Trono, D., Pedroza, A., Chovanec, L. B., Morizot, D. C., Nairn, R. S., Walter, R. B. (2001) Genetic analysis of neoplasia induced by N-nitroso-N-methylurea in Xiphophorus hybrid fish. *Mar Biotechnol (NY)*. 3, 37-43.
- Kim, S-T., Sancar, A. (1993) Photochemistry, photophysics, and mechanisms of pyrimidine dimer repair by DNA photolyase. *Photochem. Photobiol*. 57,895-904.
- Kosswig, C. (1928) Über Bastarde der Teleostier *Platyocilus* und *Xiphophorus*. *Z Indukt Abstammungs-Vererbungs*. 44, 150–158.
- Lee, J. H., Bae, S. H., Choi, B. S. (2000) The Dewar photoproduct of thymidylyl(3'-->5')-thymidine (Dewar product) exhibits mutagenic behavior in accordance with the "A rule". *Proc Natl Acad Sci U S A*. 97, 4591-4596.
- Ley, R. D. (1984) Photorepair of pyrimidine dimers in the epidermis of the marsupial *Monodelphis domestica*. *Photochem. Photobiol*. 40, 141-143.
- Li, J., T. Uchida, T. Todo & T. Kitagawa 2006 Similarities and differences between cyclobutane pyrimidine photolyase and (6-4) photolyase as revealed by resonance Raman spectroscopy. *J. Biol. Chem*. 281, 25551-25559.
- Maverakis, E., Miyamura, Y., Bowen, M. P., Correa, G., Ono, Y., Goodarzi, H. (2010) Light, including ultraviolet. *J Autoimmun*. 34, 247-257.

- McKenzie, R. L. , Björn, L. O., Bais, A., Ilyasad, M. (2003). Changes in biologically active ultraviolet radiation reaching the Earth's surface. *Photochem Photobiol Sci.* 2, 5-15.
- Mitchell, D. L., Narin, R. S. (1989) The biology of the (6-4) photoproduct. *Photochem Photobiol.* 49, 805-19.
- Mitchell, D. L., Fernandez, A. A., Nairn, R. S, Garcia, R., Paniker, L., Trono, D., Thames, H. D., Gimenez-Conti, I. (2010) Ultraviolet A does not induce melanomas in a *Xiphophorus* hybrid fish model. *Proc Natl Acad Sci U S A.* 107, 9329-9334.
- Mitchell, D., Paniker, L., Sanchez, G., Trono, D., Nairn, R. (2007) The etiology of sunlight-induced melanoma in *Xiphophorus* hybrid fish. *Mol Carcinog.* 46, 679-684.
- Mitchell, D. L., Meador, J. A., Byrom, M., Walter, R. B. (2001) Resolution of UV-induced DNA damage in *Xiphophorus* fishes. *Mar Biotechnol (NY).* 3, 61-71.
- Mitchell, D. L., Nairn, R. S., Johnston, D. A., Byrom, M., Kazianis, S., Walter, R. B. (2004) Decreased levels of (6-4) photoproduct excision repair in hybrid fish of the genus *Xiphophorus*. *Photochem Photobiol.* 79, 447-452.
- Mitchell, D. L., Paniker, L., Douki, T. (2009) DNA damage, repair and photoadaptation in a *Xiphophorus* fish hybrid. *Photochem Photobiol.* 85, 1384-1390.
- Mitchell, D. L. (2006) Quantification of photoproducts in mammalian cell DNA using radioimmunoassay. *Methods Mol Biol.* 314, 239-249.

- Mitchell, D. L., Scoggins, J. T., Morizot, D. C. (1993) DNA repair in the variable platyfish (*Xiphophorus variatus*) irradiated in vivo with ultraviolet B light. *Photochem Photobiol.* 58, 455-459.
- Nairn, R. S, Kazianis, S., Della Coletta, L., Trono, D., Butler, A. P., Walter, R. B., Morizot, D. C. (2001) Genetic analysis of susceptibility to spontaneous and UV-induced carcinogenesis in *Xiphophorus* hybrid fish. *Mar Biotechnol (NY)*. 3, 24-36.
- López-Camarillo, C., Ocampo, E. A., Casamichana, M. L., Pérez-Plasencia, C., Alvarez-Sánchez, E., Marchat, L. A. (2012) Protein Kinases and Transcription Factors Activation in Response to UV-Radiation of Skin: Implications for Carcinogenesis. *Int J Mol Sci.* 13, 142-172.
- Pettijohn, D., and Hanawalt, P. (1964) Evidence for repair-replication of ultraviolet damaged DNA in bacteria. *J Mol Biol* 9:395–410.
- Rass, K., Reichrath, J. (2008) UV damage and DNA repair in malignant melanoma and nonmelanoma skin cancer. *Adv Exp Med Biol.* 624, 162-178.
- Rigel, D. S., Kopf, A.W., Friedman, R.J. (1987) The rate of malignant melanoma in the United States: are we making an impact? *J Am Acad Dermatol.* 17, 1050-3.
- Sancar, A. (1996) No “end of history” for photolyases. *Science* 272, 48-49.
- Sancar, G. B., Sancar, A. (2006) Purification and characterization of DNA photolyases. *Methods Enzymol.* 408, 121-56.

- Schul, W., Jans, J., Rijksen, Y. M., Klemann, K. H., Eker, A. P., de Wit, J., Nikaido, O., Nakajima, S., Yasui, A., Hoeijmakers, J. H., van der Horst, G. T. (2002) Enhanced repair of cyclobutane pyrimidine dimers and improved UV resistance in photolyase transgenic mice. *EMBO J.* 21, 4719-4729.
- Setlow, R. B., Carrier, W. L. (1964). The disappearance of thymine dimers from DNA: An error-correcting mechanism. *Proc Natl Acad Sci U S A.* 51, 226-31.
- Setlow, R. B., Setlow, R. K. (1962) Evidence that ultraviolet-induced thymine dimers in DNA cause biological damage. *Proc Natl Acad Sci U S A.* 48, 1250-1257.
- Setlow, R. B., Regan, J. D., German, J., Carrier, W. L. (1969) Evidence that xeroderma pigmentosum cells do not perform the first step in the repair of UV damage to their DNA. *Proc Natl Acad Sci USA* 64, 1035– 1041.
- Tibbetts, R. S., Brumbaugh, K. M., Williams, J. M., Sarkaria, J. N., Cliby, W. A., Shieh, S. Y., Taya, Y., Prives, C., Abraham, R. T. (1999) A role for ATR in the DNA damage-induced phosphorylation of p53. *Genes Dev.* 13, 152-157.
- Tyrell, R. M. (1996) Activation of mammalian gene expression by the UV component of sunlight-from models to reality. *Bioessays* 18, 139-148.
- Wang, S. Y., (1976) Ed., *Photochemistry and photobiology of nucleic acids*, Vols I and II, Academic Press, New York.
- Wang, H. T., Choi, B., Tang, M. S. (2010) Melanocytes are deficient in repair of oxidative DNA damage and UV-induced photoproducts. *Proc Natl Acad Sci U S A.* 107, 12180-12185.

Ziegler, A., Leffell, D. J., Kunala, S., Sharma, H. W., Gailani, M., Simon, J. A., Halperin, A. J., Baden, H. P., Shapiro, P. E., Bale, A. E., Brash, D., E. (1993) Mutation hotspots due to sunlight in the p53 gene of nonmelanoma skin cancers. Proc Natl Acad Sci U S A. 90, 4216-4220.

VITA

Kevin Peter Downs was born in Providence, Rhode Island, on September 25th, 1988. After completing his work at Brazoswood High School, Lake Jackson, Texas, he entered Texas State University-San Marcos during the fall 2007. In May 2011 he earned the degree of Bachelor of Science in Biology and in May 2013 he earned the degree Master of Science in Biochemistry.

Mailing Address: 168 Spring Branch Loop

Kyle TX, 78640

This thesis was typed by Kevin P. Downs.